Published in final edited form as:
J Med Chem. 2009 January 8; 52(1): 62–73. doi:10.1021/jm800817h.

Synthesis, Radiosynthesis, and Biological Evaluation of Carbon-11 and Fluorine-18 Labeled Reboxetine Analogs: Potential Positron Emission Tomography Radioligands for in Vivo Imaging of the Norepinephrine Transporter

Fanxing Zeng[†], **Jiyoung Mun**[†], **Nachwa Jarkas**[†], **Jeffrey S. Stehouwer**[†], **Ronald J. Voll**[†], **Gilles D. Tamagnan**[‡], **Leonard Howell**[⊥], **John R. Votaw**[†], **Clinton D. Kilts**[§], **Charles B. Nemeroff**[§], and **Mark M. Goodman**[†,§,*]

[†]Department of Radiology, Emory University, Atlanta, GA 30322

[§]Department of Psychiatry and Behavioral Sciences, Emory University, Atlanta, GA 30322

[⊥]Yerkes Regional Primate Research Center, Emory University, Atlanta, GA 30322

[‡]Institute for Degenerative Diseases, New Haven, CT 06520

Abstract

Reboxetine analogs with methyl and fluoroalkyl substituents at position 2 of the phenoxy ring **1–4** were synthesized. In vitro competition binding demonstrated that **1–4** have a high affinity for the norepinephrine transporter (NET) with K_i's = 1.02, 3.14, 3.68, and 0.30 nM (vs [^{3}H]nisoxetine), respectively. MicroPET imaging in rhesus monkeys showed that the relative regional distribution of [^{11}C]**1** and [^{11}C]**4** is consistent with distribution of the NET in the brain, while [^{18}F]**2** and [^{18}F]**3** showed only slight regional differentiation in brain uptake. Especially, the highest ratios of uptake of [^{11}C]**1** in NET-rich regions to that in caudate were obtained at 1.30–1.45 at 45 min, and remained relatively constant over 85 min. Pretreatment of the monkey with the selective NET inhibitor, desipramine, decreased the specific binding for both [^{11}C]**1** and [^{11}C]**4**. PET imaging in awake monkeys suggested that anesthesia influenced the binding potential of [^{11}C]**1** and [^{11}C]**4** at the NET.

Introduction

The norepinephrine transporter (NET[a]) is a member of the Na^+/Cl^- -dependent neurotransmitter transporter gene family, located on the nerve terminals as well as the cell bodies of noradrenergic neurons. The principal physiological function of the NET is to terminate the action of the norepinephrine (NE) by removing NE from the synaptic cleft and returning it to the presynaptic neuron where the neurotransmitter can be degraded or retained for re-release at a later time.[1,2] The locus coeruleus (LC), a dense cluster of neurons in the brain stem, possesses the greatest density of NET binding sites in the mammalian brain. The major targets of noradrenergic afferents include the thalamus, hypothalamus, brain stem, amygdala, cerebral cortex, hippocampus, and cerebellum.[3–5] The location of noradrenergic

*To whom correspondence should be addressed. Address: Department of Radiology, 1364 Clifton Road NE, Atlanta, GA 30322. Phone: (404) 727-9366. Fax: (404) 727-3488. E-mail: mgoodma@emory.edu.

[a]Abbreviations: PET, positron emission tomography; SPECT, single photon emission computerized tomography; NET, norepinephrine transporter; DAT, dopamine transporter; SERT, serotonin transporter; NE, norepinephrine; SUV, standard uptake value; TAC, time-activity curve; nM, nanomolar; SPE, solid-phase extraction; TFA, trifluoroacetic acid; HRRT, highresolution research tomography; TLC, thin-layer chromatography; EI, electron ionization.

nerve terminals in these brain regions implies the presence of NET protein, and all of these regions demonstrate appreciable binding of NET selective radioligands. The lowest densities of brain NETs have been demonstrated in the occipital cortex and striatum, supporting their use as reference regions.[3] Dysregulation of noradrenergic function has been implicated in the pathophysiology of psychiatric disorders including depression, anxiety, and attention-deficit/hyperactivity disorder (ADHD), as well as neurodegenerative disorders including Alzheimer's disease and Parkinson's disease.[6–9] Therefore, development of a selective radioligand for visualization and quantification of the brain NET density using in vivo positron emission tomography (PET) or single photon emission computerized tomography (SPECT) would provide more insights as to the role of noradrenergic mechanisms in neuropsychiatric disorders as well as to the in vivo pharmacokinetic and pharmacodynamic properties of potential medications with affinity for the NET.

The quantitative mapping of brain dopamine transporters (DAT) and serotonin transporters (SERT) has novelly informed pathophysiology and pharmacotherapy of CNS disorders due to the availability of valid radioligands. In contrast, in vivo brain imaging of NET has been hampered by lack of a suitable radioligand for many years, and only recent progress has lead to useful NET radioligands. Several potent NET-selective reuptake inhibitors, such as [^{11}C]desipramine ([^{11}C]DMI)[10,11] and its hydroxylated derivative ((*R*)-[^{11}C]OHDMI),[12] nisoxetine ([^{11}C]NXT)[13] and its derivatives ([^{125}I]INXT[14] and [^{125}I]PYINXT[15]), [^{11}C]thionisoxetine,[16] [^{11}C]oxaprotiline,[13] [^{11}C]lortalamine,[13] [^{11}C]talopram,[10,17] and [^{11}C]talsupram[10,17] have been synthesized and evaluated for *in vitro* or *in vivo* mapping of brain NET. Unfortunately, these radioligands are far from ideal as selective brain imaging agents for NET. The common limitations have been high nonspecific binding, unfavorably slow kinetics, low brain uptake or poor in vivo selectivity.

The development of an ideal radiotracer to image the NET is challenging due to the low density and widespread distribution of NET-binding sites in the brain. The desirable properties for a candidate NET radioligand include (a) high binding affinity for the NET and high selectivity versus the SERT and DAT; (b) moderate lipophilicity usually lying in the log $P_{7.4}$ range 1–3 for good initial brain entry and low non-specific binding; (c) high ratios of uptake in NET-rich regions to caudate of ≥ 1.5 in non-human primates to provide a clear image of NET; (d) specific binding to brain NET reaching peak equilibrium during PET measurement to allow quantification of NET occupancy; (e) lack of radiolabeled metabolites in the brain; (f) high stability in plasma.

In the past few years, there has been extensive research on the development of analogs of reboxetine, an antidepressant selective for the NET, and more success has been achieved. Several carbon-11, fluorine-18 and iodine-123 labeled radioligands have been developed and evaluated as potential PET and SPECT NET imaging agents[13, 18–25] (Figure 1). (*S,S*)-[^{11}C]MeNER,[18–20,26,27] an *O*-methyl derivative of reboxetine, has shown a high hypothalamus-to-striatum uptake ratio of 2.5 at 60 min post injection in rats. PET imaging studies in cynomolgus monkeys and in baboons with the same ligand demonstrated that the relative regional distribution of the radioactivity is consistent with the known distribution of NET with thalamus-to-striatum uptake ratios of 1.4–1.6. Although (*S,S*)-[^{11}C]MeNER exhibited many desired in vivo properties that have not been observed with other ^{11}C-labeled NET ligands, this radioligand still has some limitations. Previous evaluation of (*S,S*)-[^{11}C]MeNER has shown that specific binding to brain NET did not reach peak equilibrium during a 90 min PET measurement. This, together with its relatively noisy signal at later time points hamper its utility in the quantitative assessment of NET binding occupancy in brain. *O*-fluoromethyl, and *O*-fluoroethyl analogs, (*S,S*)-[^{18}F]FMeNER-D_2[21] and (*S,S*)-[^{18}F]FRB-D_4[25], were then synthesized to take advantage of the longer half-life of ^{18}F. (*S,S*)-[^{18}F]FMeNER-D_2 has shown a thalamus-to-striatum binding ratio of ~1.5 in PET imaging studies in cynomolgus monkeys

and human, comparable to the ratio reported for (*S*,*S*)-[^{11}C]MeNER. Also, a specific binding peak equilibrium was obtained during the PET experiment at a lower noise level. However, although deuterium substitution on the fluoroalkyl side chain helped to reduce defluorination, in vivo defluorination was not totally inhibited and high skull uptake of radioactivity, especially in the late phases of image acquisition, was observed, an effect found to contaminate images in cortical areas in PET studies.[22,28]

As part of ongoing research in our laboratories to develop NET-specific PET imaging agents, the promising results from the reboxetine motif promoted us to continue to explore reboxetine analogs as PET NET ligands. Since in the reboxetine series, the most NET active isomer always corresponds to the *S*,*S* isomer, we decided to focus our effort on the *S*,*S* isomer. We have been exploring the incorporation of alkyl-containing substituents at position 2 of the phenoxy ring (Figure 1). We report here the synthesis and *in vitro* evaluation of (2*S*,3*S*)-2-[α-(2-methylphenoxy)phenylmethyl]morpholine (MENET, **1**), (2*S*,3*S*)-2-[α-(2-(2-fluoroethyl) phenoxy)phenylmethyl]morpholine (FENET, **2**), and (2*S*,3*S*)-2-[α-(2-(3-fluoropropyl) phenoxy)phenylmethyl]morpholine (FPNET, **3**) as well as the radiolabeling and in vivo microPET imaging of [^{11}C]**1**, [^{18}F]**2** and [^{18}F]**3** in anesthetized nonhuman primates and the PET imaging of [^{11}C]**1** in an awake nonhuman primate. Additionally, we replaced the oxygen atom by sulfur as the linker of the three rings in MENET **1** to see if this modification might provide a candidate with improved NET binding properties. To this end, we synthesized (2*S*, 3*S*)-2-[α-(2-methylphenylthio)phenylmethyl]morpholine (MESNET, **4**) and explored the microPET and PET properties of [^{11}C]**4** in nonhuman primates. Recently, the synthesis and monoamine transporter affinity have been reported for arylthiomethyl morpholine analogs of reboxetine.[29,30]

Chemistry

The stereoselective synthesis of ligands **1, 2, 3**, and **4** is shown in Scheme 1. The key intermediates **5** and **6** were synthesized in good yields and 99% enatiomeric excess in 6 linear steps starting from commercially available (*S*)-3-amino-1,2-propanediol according to a recently reported procedure.[31] 2*S*,3*S*-isomer (**5**) was the major isomer and 2*S*,3*R*-isomer (**6**) was the minor isomer. Although ether **8** could be prepared by reacting **6** with 2-methylphenol under Mitsunobu conditions, in this case the yield of **8** was below 60%. Alternatively, nucleophilic aromatic substitution of sodium alkoxide of isomer **5** with chromium tricarbonyl complex **7** followed by iodine-induced dechromination provided **8** in 95% yield without affecting the configuration at the benzylic position. The subsequent de-Boc with excess CF_3COOH yielded **1** in 79% yield. Tricarbonylchromium complex **7** was prepared in 43% yield by refluxing 2-fluorotoluene with $Cr(CO)_6$ in a mixture of dibutyl ether and THF.[32]

2-(2-Fluoroethyl)phenol (**9**) was synthesized in 40% yield by fluorination of 2-hydroxyphenethyl alcohol with diethylaminosulfur trifluoride (DAST).[33] 2-(3-Fluoropropyl) phenol (**10**) was prepared in 32% yield starting from 2-allylphenol in 4 steps according to a previously described procedure with some modification involving protection of the phenol with chloromethylmethyl ether (MOMCl), hydroboration-oxidation, fluorination of the resulting alcohol, and deprotection of the MOM group.[33] Reacting **6** with **9** and **10** under Mitsunobu conditions gave fluoroethyl compound **11** and fluoropropyl compound **12** in good yields, respectively, which then underwent cleavage of the Boc group with excess trifluoroacetic acid to afford **2** and **3**, respectively. Treatment of the alcohol **5** with carbon tetrabromide and triphenylphosphine gave (2*S*,3*R*)-*N*-*Boc*-2-[α-bromo(phenyl)methyl] morpholine (**13**) in 75% yield.[30] MESNET (**4**) was prepared by reacting 2-methylbenzenethiol with bromide **13** in DMF using Cs_2CO_3 as base followed by standard deprotection with CF_3COOH.

The synthesis of tin compounds **15** and **16**, required as precursors for radiolabeling with [^{11}C] iodomethane for [^{11}C]**1** and [^{11}C]**4**, and tosylates **17** and **18**, required as precursors for radiolabeling with [^{18}F]fluoride for [^{18}F]**2** and [^{18}F]**3**, respectively, is presented in Scheme 2 – Scheme 3. Tin precursor **15** was prepared by palladium-catalyzed stannylation of iodo compound **17**[24], easily synthesized by reacting **6** with 2-iodophenol under Mitsunobu conditions with inversion of configuration. The obvious synthetic strategy for obtaining tin precursor **16** focused on the stannylation of iodo compound **18**. Numerous efforts were undertaken, but none of the conditions provided the required tin compound. The conditions that were tried included reacting with hexamethylditin using tetrakis(triphenylphosphine) palladium ($Pd(PPh_3)_4$) as catalyst in 1,2-dimethoxyethane at 80 °C, reacting with hexamethylditin using $Pd(PPh_3)_4$ in toluene at 110 °C, reacting with hexamethylditin using $Pd_2(dba)_3$ and tri(2-furyl)phosphine as catalysts in DMF at 100 °C, and reacting with *n*-BuLi then with Me_3SnCl. Alternatively, another strategy was developed which consisted of reacting bromide **13** with mercaptide anion **20** as depicted in Scheme 2. Mercaptide anion **20** (prepared in one pot from thiophenol) is a versatile precursor for the preparation of aryl sulfides and sulfones bearing an *o*-stannyl group and allowing attachment of the *o*-stannyl group prior to introduction of the aryl sulfide and sulfone.[34,35] Consequently, tin precursor **16** was obtained in 36% overall yield by treating **20** *in situ* with bromide **13**.

Compounds **23** and **24** were obtained by reacting **6** with phenols **21** and **22** under Mitsunobu conditions. The subsequent reduction of methyl ester groups with $LiAlH_4$ followed by tosylation of the resulting hydroxyl groups afforded the precursors **17** and **18** (Scheme 3).

Radiolabeling

[^{11}C]**1** and [^{11}C]**4** were prepared from N-Boc aryltrimethylstannane **15** and **16** in a two-step synthesis, respectively (Scheme 4). The first step was a palladium-catalyzed cross coupling reaction between **15** or **16** and [^{11}C]CH_3I using a modified procedure developed by Björkman *et al.*.[36] Palladium-catalyzed cross coupling reactions utilizing organostannanes, commonly referred to as Stille couplings, have been shown to be a valuable labeling method for the synthesis of compounds containing a [^{11}C]methylphenyl moiety.[36–40] Reacting **15** or **16** with [^{11}C]CH_3I at 100 °C using palladium complex generated *in situ* from $Pd_2(dba)_3$ and (o-$CH_3C_6H_4)_3P$ (1:4) together with CuCl and K_2CO_3 as cocatalysts gave us the best coupling yield. It is worthy to note that under the earlier reported reaction temperature of 60 °C,[36] or even a higher temperature of 80 °C, a great deal of unreacted [^{11}C]CH_3I was observed when analyzing the reaction mixture. Increasing the temperature to 100 °C greatly improved the radiochemical yield of coupling. Deprotection of the N-Boc group was performed by treatment with TFA at 100 °C for 7 min. Finally, the excess acid was neutralized with aqueous ammonia before HPLC purification. Dose formulation was performed through solid-phase extraction (SPE) of the radiotracer according to a previously reported procedure[41] rather than conventional rotary evaporation of HPLC fractions.

Starting with 450–550 mCi of cyclotron produced methyl iodine, typical syntheses provided 25–45 mCi (uncorrected) of [^{11}C]**1** and [^{11}C]**4** in average radiochemical yields of 38% (decay-corrected from end of $^{11}CH_3I$ synthesis) in a total synthesis time of 60 min. Analytical HPLC demonstrated that the radiolabeled products were over 98% radiochemically pure, and specific activity ranged from 0.4 to 0.9 Ci/μmol at time of injection for both compounds.

The radiolabeling of [^{18}F]**2** and [^{18}F]**3** was accomplished through reacting tosylate precursors (**17** and **18**, respectively) with [^{18}F]fluoride in the presence of Kryptofix 222 and K_2CO_3 in acetonitrile at 90 °C for 10 min followed by removal of *N*-Boc group under acidic conditions (Scheme 5). After HPLC purification, [^{18}F]**2** and [^{18}F]**3** were obtained in 6–11% radiochemical yields (decay-corrected from [^{18}F]F^-) in a synthesis time of 100 min (from the end of

bombardment). Analytical HPLC demonstrated that the radiolabeled products were over 98% radiochemically pure, and the specific activity of the products was 1.6–3.3 Ci/μmol at time of injection for both compounds.

The log *P* values of compounds **1–4** were measured according to a previously reported procedure[42] and are presented in Table 1. The lipophilicity (octanol/phosphate buffer partition), log $P_{7.4}$, is an important parameter for correlating structure with brain penetration and ligand-transporter kinetic behavior. Compound **1–4** had log $P_{7.4}$ values of 2.04, 2.00, 2.29, and 2.47, respectively, which are in the middle range of values considered acceptable for good blood-brain barrier penetration.[43] Substitution of oxygen atom by sulfur as in compound **4** increased log $P_{7.4}$ by 0.43. This effect could be explained by a decreased polarity of **4** due to the bigger size and lower electronegativity of sulfur atom compared to oxygen. Also, log $P_{7.4}$ values, as expected, increased with increasing length of the side chain as seen in compounds **2** and **3**.

In Vitro Competition Binding Assays

Reboxetine derivatives **1–4** were screened for binding to human monoamine transporters using *in vitro* competition binding assays in transfected HEK-293 cells stably expressing the human NET (hNET), human SERT (hSERT), or human DAT (hDAT) according to a previously reported procedure.[44,45] (*S*,*S*)-Reboxetine and (*S*,*S*)-MeNER were also screened under the same assay system for comparison.

[^{3}H]nisoxetine (NET ligand), [^{3}H]citalopram (SERT ligand), and [^{125}I]RTI-55 (DAT ligand) were used as radiotracers during the *in vitro* displacement experiments. The data in Table 1 indicate that MENET (**1**) displays a high affinity for the NET (K_i = 1.02 nM) and selectivity over the SERT (92 times) and DAT (321 times) comparable to the values for (*S*,*S*)-MeNER. Compared to the methyl derivative (**1**), incorporation of ω-fluoroalkyl group at the 2-position of the phenoxy ring resulted in decreased affinities of the ligands for all three transporters. Consequently, fluoroethyl derivative (**2**) and fluoropropyl derivative (**3**) bind to the NET and SERT with approximately the same affinity, which is three to five times lower than that for **1**, respectively. **2** and **3** also exhibited very low affinity for the DAT (K_i > 6000). Replacing oxygen atom with sulfur as the linker afforded MESNET (**4**), which is 3.4 times more potent than **1** for the NET with a K_i = 0.30, and 6.5 times more potent for the SERT with a K_i = 14.80, while the affinity for the DAT remains in the same range as that of **1**.[46]

In Vivo Anesthetized Nonhuman Primate MicroPET Imaging

MicroPET imaging studies were performed with [^{11}C]**1,** [^{18}F]**2**, [^{18}F]**3** and [^{11}C]**4** to assess the regional brain distribution, imaging properties and in vivo selectivity of these radioligands for the NET in rhesus monkeys.

The microPET images acquired from 0 to 140 min after injection of [^{11}C]**1** showed that the regional brain accumulation of radioactivity was consistent with the distribution of the NET in the brain with high uptake occurring in the thalamus, midbrain, and pons (known NET-rich regions) and low uptake in caudate (NET-poor region). The corresponding baseline time-activity curves (TACs) of [^{11}C]**1** are presented in Figure 2. Following administration of [^{11}C]**1**, the uptake of radioactivity in the thalamus and pons peaked between 15.5–27.5 min after injection and then declined gradually with half-times for clearance from peak uptake ($T_{1/2}$) of ~105 min. The peak uptakes in the midbrain and cerebellum were achieved at 9.5–18.5 min postinjection, and at 18–35 min in caudate. Ratios of uptake of [^{11}C]**1** in thalamus, midbrain, pons, and cerebellum to that in caudate peaked at 1.30, 1.45, 1.40, and 1.30 at 45 min, respectively, and remained relatively constant at 1.30, 1.43, 1.44, and 1.25 at 85 min, indicating

that a quasiequilibrium (a condition where the ratio of radioactivity uptake in the region of interest to reference region stays relatively constant) has been established.

Imaging studies were also performed with [^{18}F]**2** and [^{18}F]**3** to take advantage of the longer half-life of ^{18}F (109.8 min). The TACs for the baseline studies with [^{18}F]**2** and [^{18}F]**3** are showed in Figure 3 and Figure 4, respectively. Compound [^{18}F]**2** and [^{18}F]**3** enter the brain rapidly and achieve peak uptake after 15 min in all regions of interest followed by a fast washout. The regional brain accumulation of [^{18}F]**2** and [^{18}F]**3** approximately matched the distribution of the NET; however, high uptakes in caudate, a region that is supposed to contain low levels of NET, were also observed. Ratios of uptake in thalamus, midbrain and cerebellum to that in caudate peaked at 1.13, 1.13, and 1.05 for [^{18}F]**2** and 1.18, 1.18, and 0.95 for [^{18}F]**3**, respectively. The slight regional differentiation in brain uptake together with the unexpected accumulation of radioactivity in the caudate makes [^{18}F]**2** and [^{18}F]**3** unpromising NET radioligands.

Although high in vitro affinity of a ligand does not guarantee its suitability as an in vivo radioligand, high affinity is the predominately important characteristics of a prospective radioligand for imaging low density of molecular target, such ad NET. The NET affinities of 3.14 and 3.68 nM for **2** and **3**, which is three to four times lower than that for **1** and MeNER, might not be high enough to show specific binding in NET-rich regions and might be attributed to the poor signal-to-noise ratio of [^{18}F]**2** and [^{18}F]**3**. No further imaging studies were performed with [^{18}F]**2** and [^{18}F]**3**.

In our extensive study on tropane and diarylsulfide motif to develop SERT-specific radioligands, we found that if a ligand's affinity for the SERT was greater than 1 nM, this ligand did not show specific binding in SERT-rich regions. We were interested to test whether compound **4** with Ki for SERT of 14.8 nM might present the same property. In addition, study on compound **4**, which is three times more potent but less selective than **1** and MeNER, might provide important structure-affinity relationship information in terms of binding and kinetics. The TACs for the baseline study with [^{11}C]**4** showed in Figure 5 indicate that the peak uptake of radioactivity in thalamus and midbrain was achieved 27.5–45 min after injection, and then washed out slowly with a $T_{1/2}$ = ~160 min. The slower binding kinetics exhibited by [^{11}C]**4** in comparison to [^{11}C]**1** may reflect a higher binding affinity of [^{11}C]**4** to the NET (Table 1). The thalamus-to-caudate and midbrain-to-caudate ratios for [^{11}C]**4** were 1.34 and 1.33 at 85 min, respectively. To assess the potential binding of [^{11}C]**4** to the SERT, chase study with SERT ligand (R,S)-citalopramHBr was performed in the same rhesus monkey. A dose of (R,S)-citalopramHBr (1.5 mg/kg) was administered 40 min after injection of [^{11}C]**4** and resulted in no displacement of radioactivity in the caudate suggesting that [^{11}C]**4** accumulation in the caudate was not due to SERT binding but most likely non-specific binding.

To demonstrate that the brain regional [^{11}C]**1** and [^{11}C]**4** binding was specific to the NET, in vivo microPET blocking studies by the NET ligand desipramine were performed. Pretreatment of monkeys with a dose of desipramine (0.125 and 0.25 mg/kg for [^{11}C]**1** and 0.125 mg/kg for [^{11}C]**4**) at 40 min prior to injection resulted in a marked reduction of radioactivity in the NET-rich brain regions: thalamus, midbrain, pons, medulla, and cerebellum, but not in caudate (Figure 6, Figure 7, and Figure 8). The reduction of ratios of [^{11}C]**1** and [^{11}C]**4** uptake in regions-of-interest to caudate at 85 min postinjection in the pretreatment studies in comparison with the baseline studies (Table 2) indicated that brain regional [^{11}C]**1** and [^{11}C]**4** uptake reflected specific NET binding.

PET Imaging in Awake Nonhuman Primates

Human PET imaging using [^{18}F]FECNT, a selective DAT radioligand, demonstrated that 1% isoflurane anesthesia increases radiotracer binding to DAT-rich brain regions, consistent with

an increase in plasma membrane expressed DAT.[47] To address the possibility of isoflurane similarly influencing the NET binding of [^{11}C]**1** and [^{11}C]**4**, PET studies were performed in awake rhesus monkeys using a high-resolution research tomography (HRRT).

The PET images were acquired for 120 min and coregistered with composite MRI images to accurately identify the regions of interest. Following administration of [^{11}C]**1**, PET images showed a clear visualization of the thalamus, locus coeruleus, midbrain, and pons (Figure 9). The resulting time-activity curves of [^{11}C]**1** presented in Figure 10 indicated that the kinetics of [^{11}C]**1** binding was not significantly altered by isoflurane anesthesia. In both awake and anesthetized monkey studies, [^{11}C]**1** reached peak uptake between 17.5–35 min and washed out gradually with similar half-times for clearance for all the regions. However, compared to anethetized monkey studies, kinetics of [^{11}C]**4** was markedly decreased in unanethetized animals with prolonged retention over the course of the imaging session indicating anesthesia influences the kinetics of [^{11}C]**4** (Figure 11). Additionally, the highest ratios of uptake in NET-rich regions relative to caudate decreased in awake monkey studies with 1.25, 1.20, 1.13, and 0.93 for the thalamus, midbrain, pons, and cerebellum, respectively, when [^{11}C]**1** was injected and 1.15, 1.0, 1.0, and 0.95, when [^{11}C]**4** was injected, suggesting that anesthesia influences the binding potential of [^{11}C]**1** and [^{11}C]**4** in these regions. The lower ratio, together with the slow binding kinetics make [^{11}C]**4** inferior to [^{11}C]**1** as a PET radioligand for NET.

So far, (*S*,*S*)-[^{11}C]MeNER is probably the most promising carbon-11 labeled PET NET radioligand. However, this ligand does not appear to be an ideal radioligand. PET examination in a cynomolgus monkey and baboons has shown that the specific binding to NET increased continuously towards the end of a PET measurement and did not reach specific binding peak equilibrium during a 90 min PET measurement.[18,20] In the present study, [^{11}C]**1** showed a greater washout and a specific binding peak equilibrium was indeed achieved in less than 1 h after injection in both anesthetized and awake states. Thurs, [^{11}C]**1** has more attractive imaging kinetic characteristics than [^{11}C]MeNER. On the other hand, [^{11}C]MeNER shows a slightly higher ratios of uptake in NET-rich brain regions to striatum of 1.4–1.6 than [^{11}C]**1** of 1.3–1.45 at 90 min postinjection. The difference in uptake ratio is a result of the difference in kinetics for each tracer. In both awake and anesthetized rhesus monkey studies, [^{11}C]**1** reached peak uptake between 17.5–35 min and washed out gradually with similar half-times for clearance for all the regions. In contrast, for [^{11}C]MeNER there was a slow clearance of radioactivity in NET-rich regions and a faster washout in striatum in both macaque and baboon species. This resulted in a continuously increasing uptake ratio with time. After analyzing baseline TACs reported for [^{11}C]MeNER in a cynomolgus monkey and a baboon, we found that thalamus-to-striatum ratio was approximately 1.3 at 45 min postinjection for both species. Although there is species and intersubject variability, this value is very similar to that obtained for [^{11}C]**1** in the present anesthetized rhesus monkey study. Therefore, [^{11}C]**1** might be more suitable for measuring NET density in human due to its superior kinetics and the ability to achieve a quasi-equilibrium.

Summary

As an effort to develop potential PET imaging agents for the human brain NET, four enatiomerically pure (*S*,*S*)-isomers of reboxetine derivatives, MENET **1**, FENET **2**, FPNET **3**, and MESNET **4**, were synthesized by incorporation of methyl and ω-fluoroalkyl groups at position 2 of the phenoxy ring. Competition binding assays in cells stably expressing the human monoamine transporters indicated that **1** had a high affinity for the NET and selectivity relative to the SERT and DAT. ω-Fluoroalkylation of **1** yielded **2** and **3** and reduced the NET and SERT affinity three to five fold. Replacing the oxygen atom with sulfur as the linker of the three rings as seen in **4** increased the NET affinity 3.4 times, but decreased the selectivity of NET over SERT to half that of **1**. All four of the candidate NET ligands exhibited low affinity for the

DAT. [^{11}C]**1** and [^{11}C]**4** were prepared by palladium catalyzed cross coupling of their N-*t*-Boc aryltrimethylstannane precursors with [^{11}C]methyl iodide followed by deprotection with TFA, while [^{18}F]**2** and [^{18}F]**3** were prepared by reacting tosylate precursors with [^{18}F]fluoride in the presence of Kryptofix 222 and K_2CO_3. Tracers [^{11}C]**1**, [^{18}F]**2**, [^{18}F]**3**, and [^{11}C]**4** were found to have lipophilicities in the range log $P_{7.4}$ = 2.00–2.47. In vivo microPET imaging studies in a rhesus monkey showed that [^{11}C]**1** and [^{11}C]**4** displayed high uptake in the thalamus, midbrain, pons, and cerebellum, and low uptake in caudate, a pattern consistent with distribution of the NET in the brain. After injection of [^{11}C]**1**, a specific binding peak equilibrium was obtained with the highest ratios of uptake in the thalamus and midbrain to that in caudate of 1.30 and 1.45 at 45 min, respectively. [^{11}C]**4** showed slower binding kinetics relative to [^{11}C]**1**. Desipramine pretreatment studies with [^{11}C]**1** and [^{11}C]**4** confirmed the binding of these radiotracers to the monkey brain NET. Following intravenous injection of [^{18}F]**2** and [^{18}F]**3**, there was uptake of radioactivity into NET-rich regions, but only to a slightly greater extent than into caudate. In vivo PET imaging studies in awake monkeys demonstrated that [^{11}C]**1** kinetics was not significantly altered by isoflurane anesthesia, while kinetics of [^{11}C]**4** was greatly decreased. Additionally, the highest ratios of uptake in NET-rich regions relative to caudate were decreased for both [^{11}C]**1** and [^{11}C]**4**, indicating that anesthesia influenced their binding potential. Comparison between [^{11}C]**1** and [^{11}C]MeNER demonstrated that although [^{11}C]MeNER shows a slightly higher ratio of uptake in NET-rich brain regions to striatum at 90 min postinjection, [^{11}C]**1** has more attractive imaging kinetics by achieving a quasi-equilibrium in less than 1 h, suggesting [^{11}C]**1** might be useful for mapping NETs occupancy in the human brain. PET images of [^{11}C]**1** in primates under test-retest condition to assess reproducibility are currently in progress. Further experiments to examine the binding of [^{11}C]**1** to human NETs in vitro and in vivo are also underway.

Experimental Section

General

All reagents used were obtained from commercially available sources and were used without further purification. All reactions were performed in oven glassware fitted with rubber septa under argon. ^{1}H NMR spectra were recorded on a Varian spectrometer at 400 MHz and referenced to the NMR solvent (chemical shifts in ppm values, *J* values in Hz). High-resolution mass spectra were acquired on a VG 70-S double focusing mass spectrometer using electron ionization (EI). Elemental analyses of selected compounds were performed by Atlantic Microlab (Norcross, GA). Thin-layer chromatography (TLC) was performed using 250 μm layers of F-254 silica on aluminum plates obtained from Whatman (Clifton, NJ) and visualized by UV light. Flash chromatography was carried out using Merck silica gel 60 (40–63 μm particle size).

Chemistry. (2*S*,3*S*)-*N*-*tert*-Butoxycarbonyl-2-[α-(2-methylphenoxy)phenylmethyl] morpholine (8)

To a suspension of NaH (60% oil dispersion, 15 mg, 0.375 mmol) in DMF (0.8 mL) was added dropwise (2*S*,3*S*)-N-Boc-2-[α-hydroxy(phenyl)methyl]morpholine (**5)** (75 mg, 0.25 mmol) in DMF (1.5 mL) at room temperature under Ar. After 1 h η^6-(2-fluorotoluene) tricarbonylchromium (**7)** (92 mg, 0.375 mmol) in DMF (1.5 mL) was added to the reaction mixture. The mixture was stirred for 2 h at room temperature and then cooled to 0 °C before addition of a solution of I_2 (390 mg, 1.53 mmol) in THF (2 mL) dropwise. The whole mixture was stirred for 30 min at room temperature, and then 10 mL of 10% $Na_2S_2O_3$ solution was added. The mixture was extracted three times with EtOAc, and the extracts were combined and washed twice with H_2O. The organic layer was dried over Na_2SO_4 and the solvent was evaporated under reduced pressure. The crude product was purified by flash chromatography on silica eluted with hexane/EtOAc (80:20) to afford **8** as colorless oil (91 mg, 95%): ^{1}H NMR

($CDCl_3$, 400 MHz), δ 7.25–7.37 (m, 5H), 7.10–7.11 (m, 1H), 6.94–6.98 (m, 1H), 6.77–6.80 (m, 1H), 6.62–6.64 (m, 1H), 5.19 (m, 1H), 3.91 (m, 4H), 3.55 (t, *J* = 11.0 Hz, 1H), 2.89 (m, 1H), 2.71 (m, 1H), 2.33 (s, 3H), 1.42 (s, 9H); ^{13}C NMR ($CDCl_3$, 100 MHz), δ 156.1, 155.0, 137.5, 130.9, 128.7, 128.4, 127.2, 126.8, 121.0, 113.3, 81.6 (br), 80.2, 78.1, 66.9, 45.8, 44.5, 28.5, 16.7. HRMS $[MH]^+$ Calcd for $C_{23}H_{30}O_4N$: 384.2169, Found: 384.2168.

(2*S*,3S)-2-[α-(2-Methylphenoxy)phenylmethyl]morpholine (MENET, 1)

Trifluoroacetic acid (0.27 mL, 3.56 mmol) was added dropwise to a solution of **8** (91 mg, 0.24 mmol) in CH_2Cl_2 (3 mL) at 0 °C. The reaction mixture was allowed to reach room temperature and stirred for another 2 h. 6 mL of 1 M NaOH solution was then slowly added at 0 °C and the mixture was extracted with CH_2Cl_2. The extracts were combined, dried over Na_2SO_4, and the solvent was evaporated under reduced pressure. The crude product was purified by flash chromatography on silica eluted with MeOH/CH_2Cl_2 (10:90) to afford **1** as colorless oil (53 mg, 79%): ^{1}H NMR ($CDCl_3$, 400 MHz), δ 7.34–7.35 (m, 2H), 7.29–7.32 (m, 2H), 7.24–7.27 (m, 1H), 7.08–7.09 (m, 1H), 6.93–6.96 (m, 1H), 6.75–6.78 (m, 1H), 6.64–6.66 (m, 1H), 5.11 (d, *J* = 5.8 Hz, 1H), 3.88–3.95 (m, 2H), 3.64 (dt, *J* = 11.2, 2.9 Hz, 1H), 2.75 –2.83 (m, 2H), 2.65–2.67 (m, 1H), 2.57–2.61 (m, 1H), 2.31 (s, 3H), 1.79 (s, br, 1H); ^{13}C NMR ($CDCl_3$, 100 MHz), δ 156.3, 138.1, 130.9, 128.6, 128.2, 127.7, 127.3, 126.7, 120.9, 113.6, 81.4, 79.5, 68.5, 47.7, 46.0, 16.8. HRMS $[MH]^+$ Calcd for $C_{18}H_{22}O_2N$: 284.1645, Found: 284.1646. Anal. ($C_{18}H_{21}O_2N$) C, H, N.

η^6-(2-Fluorotoluene)tricarbonylchromium (7)

A mixture of 2-fluorotoluene (550 mg, 5 mmol) and chromium hexacarbonyl (1.65 g, 7.5 mmol) in di-*n*-butyl ether (35 mL) and THF (1.5 mL) was reflux for 60 h under argon. After evaporation of the solvent under reduced pressure, the crude product was purified by flash chromatography on silica eluted with hexane/EtOAc (80:20) to afford **7** as a yellow crystalline solid (530 mg, 43%): ^{1}H NMR (DMSO-d_6, 400 MHz), δ 6.05–6.08 (m, 1H), 5.96–6.00 (m, 1H), 5.77 (m, 1H), 5.35–5.38 (m, 1H), 2.16 (s, 3H).

(2*S*,3*S*)-*N-tert*-Butoxycarbonyl--2-[α-(2-(2-fluoroethyl)phenoxy)phenylmethyl]morpholine (11)

To a mixture of **6** (60 mg, 0.2 mmol), 2-(2-fluoroethyl)phenol (**9**) (52 mg, 0.4 mmol), and triphenylphosphine (108 mg, 0.4 mmol) in dry THF (4 mL) was added diisopropyl azodicarboxylate (79 μL, 0.4 mmol) at 0 °C. The reaction mixture was allowed to reach room temperature and stirred for 24 h. The crude product was concentrated under reduced pressure and was loaded on a short silica column eluted with hexane/EtOAc (85:15), and 100 mL fractions were colleted. After evaporating the solvent, colorless oil (64 mg) was obtained, and NMR shows it is the mixture of **11** and **9** (3:1), which was used without any further purification.

(2*S*,3*S*)-2-[α-(2-(2-Fluoroethyl)phenoxy)phenylmethyl]morpholine (FENET, 2)

Trifluoroacetic acid (0.18 mL, 2.33 mmol) was added dropwise to a solution of **11** (48 mg, 0.116 mmol) obtained as above in CH_2Cl_2 (3 mL) at 0 °C. The reaction mixture was allowed to reach room temperature and stirred for another 2 h. 4 mL of 1 M NaOH solution was then slowly added at 0 °C and the mixture was extracted with CH_2Cl_2. The extracts were combined, dried over Na_2SO_4, and the solvent was evaporated under reduced pressure. The crude product was purified by flash chromatography on silica eluted with MeOH/CH_2Cl_2 (10:90) to afford **2** as colorless oil (25 mg, 40% in two-step): ^{1}H NMR ($CDCl_3$, 400 MHz), δ 7.26–7.34 (m, 5 H), 7.14 (dd, *J* = 1.6, 7.3 Hz, 1H), 7.01 (td, *J* = 1.6, 7.9 Hz, 1H), 6.81 (td, *J* = 0.9, 7.3 Hz, 1H), 6.68 (d, *J* = 7.9 Hz, 1H), 5.07 (d, *J* = 6.3 Hz, 1H), 4.70–4.77 (m, 1H), 4.61 (m, 1H), 3.85–3.95 (m, 2H), 3.65 (td, *J* = 3.8, 10.1 Hz, 1H), 3.16 (t, *J* = 7.0 Hz, 1H), 3.11 (t, *J* = 7.0 Hz, 1H), 2.78–2.82 (m, 2H), 2.52–2.57 (m, 2H), 1.79 (s, br, 1H); ^{13}C NMR ($CDCl_3$, 100 MHz), δ 156.4,

137.8, 131.1, 128.8, 128.5, 128.0, 127.2, 125.9 (d, $J_{C–F}$ = 7.6 Hz), 121.0, 113.6, 83.4 (d, $J_{C–F}$ = 167.1 Hz), 81.8, 79.5, 68.3, 47.7, 46.0, 32.2 (d, $J_{C–F}$ = 21.4 Hz). HRMS $[MH]^+$ Calcd for $C_{19}H_{23}FNO_2$: 316.1707, Found: 316.1707. Anal. ($C_{19}H_{22}FNO_2$) C, H, N.

(2*S*,3*S*)-*N-tert*-Butoxycarbonyl-2-[α-(2-(3-fluoropropyl)phenoxy)phenylmethyl]morpholine (12)

To a mixture of **6** (60 mg, 0.2 mmol), 2-(3-fluoropropyl)phenol (**10**) (58 mg, 0.4 mmol), and triphenylphosphine (108 mg, 0.4 mmol) in dry THF (4 mL) was added diisopropyl azodicarboxylate (79 μL, 0.4 mmol) at 0 °C. The reaction mixture was allowed to reach room temperature and stirred for 24 h. The crude product was concentrated under reduced pressure and was loaded on a short silica column eluted with hexane/EtOAc (85:15), and 100 mL fractions were colleted. After evaporating the solvent, colorless oil (72 mg) was obtained, and NMR shows it is the mixture of **12** and **10** (3.5:1), which was used without any further purification.

(2*S*,3*S*)-2-[α-(2-(3-Fluoropropyl)phenoxy)phenylmethyl]morpholine (FPNET, 3)

Trifluoroacetic acid (0.19 mL, 2.48 mmol) was added dropwise to a solution of **12** (56 mg, 0.13 mmol) obtained as above in CH_2Cl_2 (3 mL) at 0 °C. The reaction mixture was allowed to reach room temperature and stirred for another 2 h. 4 mL of 1 M NaOH solution was then slowly added at 0 °C and the mixture was extracted with CH_2Cl_2. The extracts were combined, dried over Na_2SO_4, and the solvent was evaporated under reduced pressure. The crude product was purified by flash chromatography on silica eluted with MeOH/CH_2Cl_2 (10:90) to afford **3** as colorless oil (29 mg, 44% in two-step): ^{1}H NMR ($CDCl_3$, 400 MHz), δ 7.30–7.35 (m, 4H), 7.26–7.28 (m, 1H), 7.10 (dd, *J* = 1.6, 7.3 Hz, 1H), 6.97 (td, *J* = 1.4, 8.1 Hz, 1H), 6.79 (td, *J* = 0.9, 8.1 Hz, 1H), 6.65 (d, *J* = 8.1 Hz, 1H), 5.07 (d, *J* = 6.2 Hz, 1H), 4.52 (td, *J* = 2.3, 5.7 Hz, 1H), 4.44 (td, *J* = 2.4, 5.7 Hz, 1H), 3.91–3.93 (m, 1H), 3.86–3.90 (m, 1H), 3.64 (td, *J* = 2.9, 11.3 Hz, 1H), 2.75–2.83 (m, 4H), 2.54–2.63 (m, 2H), 2.01–2.10 (m, 2H), 1.82 (s, br, 1H); ^{13}C NMR ($CDCl_3$, 100 MHz), δ 156.2, 137.9, 130.4, 130.3, 128.7, 128.3, 127.3, 127.2, 120.9, 113.5, 84.0 (d, $J_{C–F}$ = 165.9 Hz), 81.5, 79.5, 68.3, 47.6, 46.0, 30.9 (d, $J_{C–F}$ = 18.7 Hz), 26.6 (d, $^1J_{C–F}$ = 18.7 Hz). HRMS $[MH]^+$ Calcd for $C_{20}H_{25}FNO_2$: 330.1864, Found: 330.1859. Anal. ($C_{20}H_{24}FNO_2$) C, H, N.

(2*S*,3*R*)-*N-tert*-Butoxycarbonyl-2-[α-bromo(phenyl)methyl]morpholine (13)

To a solution of **5** (118 mg, 0.4 mmol) in CH_2Cl_2 (3 mL) was added PPh_3 (210 mg, 0.8 mmol) at room temperature. The mixture was then cooled down to 0 °C, and a solution of CBr_4 (266 mg, 0.8 mmol) in CH_2Cl_2 (1 mL) was then added dropwise at this temperature. The reaction mixture was warmed up to room temperature and stirring was continued for 30 min. The solvent was evaporated and the crude product was purified by flash chromatography on silica eluted with hexane/EtOAc (80:20) to afford **13** as colorless oil (107 mg, 75%): ^{1}H NMR ($CDCl_3$, 400 MHz), δ 7.26–7.41 (m, 5H), 4.84 (d, *J* = 7.6 Hz, 1H), 4.36 (s, br, 1H), 3.79–3.86 (m, 3H), 3.46 (td, *J* = 2.8, 11.4 Hz, 1H), 2.92–2.96 (m, 2H), 1.46 (s, 9H); ^{13}C NMR ($CDCl_3$, 100 MHz), δ 154.8, 138.7, 128.8, 128.6, 80.5, 77.9, 66.9, 53.3, 47.0 (br), 43.2 (br), 28.6. HRMS $[MH]^+$ Calcd for $C_{16}H_{23}O_3N^{79}Br$: 356.0856, Found: 356.0854.

(2*S*,3*S*)-*N-tert*-Butoxycarbonyl-2-[α-(2-methylphenylthio)phenylmethyl]morpholine (14)

A reaction mixture of **13** (28 mg, 0.08mmol), 2-methylbenzenethiol (19 μL, 0.16 mmol), and Cs_2CO_3 (52 mg, 0.16 mmol) in DMF (2 mL) was stirred at room temperature for 18 h. The crude product was directly purified by flash chromatography on silica eluted with hexane/EtOAc (80:20) to afford **14** as pale yellow oil (26 mg, 84%): ^{1}H NMR ($CDCl_3$, 400 MHz), δ 7.03–7.18 (m, 9H), 4.13 (d, *J* = 7.3 Hz, 1H), 3.98–4.00 (m, 1H), 3.76 (m, br, 3H), 3.53–3.59 (m, 1H), 2.94–3.00 (m, 1H), 2.77 (m, br, 1H), 2.27 (s, 3H), 1.38 (s, 9H).

(2*S*,3*S*)-2-[α-(2-Methylphenylthio)phenylmethyl]morpholine (MESNET, 4)

Trifluoroacetic acid (0.1 mL, 1.31 mmol) was added dropwise to a solution of **14** (35 mg, 0.09 mmol) in CH_2Cl_2 (1.5 mL) at 0 °C. The reaction mixture was allowed to reach room temperature and stirred for another 2 h. 2 mL of 1 M NaOH solution was then slowly added at 0 °C and the mixture was extracted with CH_2Cl_2. The extracts were combined, dried over Na_2SO_4, and the solvent was evaporated under reduced pressure. The crude product was purified by flash chromatography on silica eluted with MeOH/CH_2Cl_2 (10:90) to afford **4** as pale yellow oil (19 mg, 72%), which was solidified in a freezer: ^{1}H NMR ($CDCl_3$, 400 MHz), δ 7.15–7.21 (m, 6H), 7.00–7.06 (m, 2H), 6.93–6.97 (m, 1H), 4.13 (d, *J* = 7.9 Hz, 1H), 4.00–4.03 (m, 1H), 3.82–3.87 (m, 1H), 3.66 (td, *J* = 2.8, 11.1 Hz, 1H), 2.87 (td, *J* = 3.2, 11.1 Hz, 1H) 2.70–2.80 (m, 1H), 2.59–2.69 (m, 2H), 2.26 (s, 3H), 2.06 (s, br, 1H); ^{13}C NMR ($CDCl_3$, 100 MHz), δ 140.7, 139.2, 133.7, 133.5, 130.2, 128.6, 128.4, 127.6, 127.3, 126.2, 79.4, 68.6, 56.6, 49.8, 45.8, 20.9. HRMS $[MH]^+$ Calcd for $C_{18}H_{22}ONS$: 300.1416, Found: 300.1414. Anal. ($C_{18}H_{21}ONS$) C, H, N.

(2*S*,3*S*)-*N-tert*-Butoxycarbonyl-2-[α-(2-iodophenoxy)phenylmethyl]morpholine (17)

To a mixture of **6** (30 mg, 0.1 mmol), 2-iodophenol (44 mg, 0.2 mmol), and triphenylphosphine (53 mg, 0.2 mmol) in dry THF (2 mL) was added diisopropyl azodicarboxylate (40 μL, 0.2 mmol) at 0 °C. The reaction mixture was allowed to reach room temperature and stirred during 48 h. The crude product was concentrated under reduced pressure and purified by flash chromatography on silica eluted with hexane/EtOAc (80:20) to afford **17** as colorless oil (32 mg, 64%): ^{1}H NMR ($CDCl_3$, 400 MHz), δ 7.72–7.74 (m, 1H), 7.25–7.38 (m, 5H), 7.06–7.11 (m, 1H), 6.60–6.62 (m, 2H), 5.30 (m, 1H), 3.86–3.94 (m, 4H), 3.54–3.60 (m, 1H), 2.80–2.90 (m, 1H), 2.70–2.75 (m, 1H), 1.42 (s, 9H). ^{13}C NMR ($CDCl_3$, 100 MHz), δ 156.1, 155.0, 139.7, 136.2, 129.4, 128.7, 128.6, 127.5, 123.0, 113.9, 82.1, 80.9, 80.2, 67.0, 44.8, 42.3, 28.6. HRMS $[MH]^+$ Calcd for $C_{22}H_{27}O_4NI$: 496.0979, Found: 496.0978.

(2*S*,3*S*)-*N-tert*-Butoxycarbonyl-2-[α-(2-trimethylstannylphenoxy)phenylmethyl]morpholine (15)

To a solution of **17** (27 mg, 0.055 mmol) in 1, 2-dimethoxyethane (2 mL) was added Pd$(PPh_3)_4$ (7 mg) and hexamethylditin (56 μL, 0.27 mmol). The mixture was purged under Ar for 15 min and then heated at 80 °C for 18 h. The solvent was evaporated and the crude product was purified by flash chromatography on silica eluted with hexane/EtOAc/Et_3N (92:8:0.1) to afford **15** as colorless oil (23 mg, 80%): ^{1}H NMR ($CDCl_3$, 400 MHz), δ 7.25–7.35 (m, 6H), 7.06–7.10 (m, 1H), 6.85–6.88 (m, 1H), 6.53 (d, *J* = 8.2 Hz, 1H), 5.14 (m, 1H), 3.90–3.92 (m, 1H), 3.71–3.80 (m, 2H), 3.61–3.65 (m, 1H), 3.50–3.56 (m, 1H), 2.87 (m, 1H), 2.61–2.67 (m, 1H), 1.55 (s, 9H), 1.40 (s, 9H).

(2*S*,3*S*)-*N-tert*-Butoxycarbonyl-2-[α-(2-iodophenylthio)phenylmethyl]morpholine (18)

A reaction mixture of **13** (71 mg, 0.2mmol), 2-iodobenzenethiol (94 mg, 0.4 mmol), and Cs_2CO_3 (130 mg, 0.4 mmol) in DMF (2 mL) was stirred at room temperature for 18h. The crude product was directly purified by flash chromatography on silica eluted with hexane/EtOAc (80:20) to afford **18** as colorless oil (65 mg, 63%): ^{1}H NMR ($CDCl_3$, 400 MHz), δ 7.45–7.47 (m, 1H), 7.13–7.27 (m, 6H), 6.92–7.02 (m, 2H), 4.41 (d, *J* = 7.3 Hz, 1H), 3.98 (d, *J* = 11.8 Hz, 1H), 3.76–3.80 (m, 3H), 3.52–3.58 (m, 1H), 2.97–3.04 (m, 1H), 2.83 (m, br, 1H), 1.38 (s, 9H).

(2*S*,3*S*)-*N-tert*-Butoxycarbonyl-2-[α-(2-trimethylstannylphenylthio)phenylmethyl] morpholine (16)

To a stirred solution of *n*-butyllithium (0.97 mL, 1.6 M in hexanes, 1.55 mmol) and tetramethylethylenediamine (0.23 mL, 1.55 mmol) in hexane (2.0 mL) at −78 °C was added

thiophenol (0.072 mL, 0.7 mmol) resulting in a clear, light yellow solution. The reaction mixture was warmed up to room temperature and stirred vigorously for 24 h resulting in an opaque, fine off-white slurry. THF (2 mL) was then added, causing the reaction mixture to turn homogeneous and light yellow. The reaction mixture was then cooled to −78 °C, and trimethyltin chloride (0.9 mL, 1 M in hexanes, 0.9 mmol) was added and stirring was continued for 1 h to afford mercaptide. **13** (107 mg, 0.3 mmol), Cs_2CO_3 (293 mg, 0.9 mmol) and DMF (3 mL) was then added to the mercaptide and the reaction mixture was heated at 100 °C overnight. The solvent was evaporated and the crude product was purified by flash chromatography on silica eluted with hexane/EtOAc/Et_3N (92:8:0.1) to afford **16** as colorless oil (59 mg, 36%): ^{1}H NMR ($CDCl_3$, 400 MHz), δ 7.30–7.32 (m, 1H), 7.15–7.21 (m, 6H), 7.08–7.10 (m, 2H), 4.17 (d, *J* = 7.3 Hz, 1H), 3.94–3.97 (dd, *J* = 1.9, 11.7 Hz, 1H), 3.64–3.84 (m, 3H), 3.52–3.58 (td, *J* = 2.6, 11.7 Hz, 1H), 2.90–2.94 (m, 1H), 2.69 (s, br, 1H), 1.39 (s, 9H), 0.27 (s, 9H). HRMS $[MH]^+$ Calcd for $C_{25}H_{36}NO_3SSn$: 550.1432, Found: 550.1432.

tert-Butyl (2*S*, 3*S*)-2-[α-(2-(2-methoxy-2-oxoethyl)phenoxy)(phenyl)methyl]morpholine-4-carboxylate (23)

To a mixture of **6** (46 mg, 0.157 mmol), methyl 2-(2-hydroxyphenyl)acetate (**21**) (52 mg, 0.31 mmol), and triphenylphosphine (81 mg, 0.31 mmol) in dry THF (3 mL) was added diisopropyl azodicarboxylate (61 μL, 0.31 mmol) at 0 °C. The reaction mixture was allowed to reach room temperature and stirred during 48 h. The crude product was concentrated under reduced pressure and purified by flash chromatography on silica eluted with hexane/EtOAc (80:20) to afford **23** as colorless oil (30 mg, 43%): ^{1}H NMR ($CDCl_3$, 400 MHz), δ 7.25–7.32 (m, 5H), 7.14–7.20 (m, 1H), 7.01–7.05 (m, 1H), 6.82–6.85 (m, 1H), 6.62 (d, *J* = 8.0 Hz, 1H), 5.14 (d, *J* = 5.7 Hz, 1H), 3.89 (dd, *J* = 1.9, 11.4 Hz, 1H), 3.65–3.79 (m, 8H), 3.52 (td, *J* = 2.8, 11.7 Hz, 1H), 2.86–2.90 (m, 1H), 2.65–2.70 (m, 1H), 1.41 (m, 9H). HRMS $[MH]^+$ Calcd for $C_{25}H_{32}NO_6$: 442.2224, Found: 442.2223.

tert-Butyl (2*S*, 3*S*)-2-[α-(2-(2-hydroxyethyl)phenoxy)(phenyl)methyl]morpholine-4-carboxylate (25)

To a solution of **23** (38 mg, 0.086 mmol) in dry ether (4 mL) was added $LiAlH_4$ (15 mg, 0.4 mmol) at 0 °C. After the mixture was stirred at 0 °C for 30 min the reaction was quenched by slow addition of 0.3 mL of H_2O, followed by 0.3 mL of 20% aqueous NH_4Cl, and finally 0.6 mL of H_2O. The suspension was stirred until a fine grey suspension formed, which was then vacuum filtered, and the supernatant was dried over $MgSO_4$. The solution was filtered and concentrated. Purification by flash chromatography (hexane:EtOAc 50:50) gave a colorless oil (23 mg, 64%): ^{1}H NMR ($CDCl_3$, 400 MHz), δ 7.29–7.38 (m, 5H), 7.12 (dd, *J* = 1.6, 7.3 Hz, 1H), 6.98 (td, *J* = 1.6, 7.6 Hz, 1H), 6.82 (td, *J* = 1.0, 7.3 Hz, 1H), 6.62 (d, *J* = 8.3 Hz, 1H), 5.11 (d, *J* = 6.3 Hz, 1H), 3.91–3.96 (m, 2H), 3.78–3.87 (m, 3H), 3.55 (td, *J* = 2.8, 11.7 Hz, 1H), 3.09–3.15 (m, 1H), 2.87–2.96 (m, 2H), 2.67–2.73 (m, 2H), 1.39 (s, 9H). HRMS $[MH]^+$ Calcd for $C_{24}H_{32}NO_5$: 414.2275, Found: 414.2282.

tert-Butyl (2*S*, 3*S*)-2-[α-(2-(2-tosyloxyethyl)phenoxy)(phenyl)methyl]morpholine-4-carboxylate (17)

A solution of **25** (20 mg, 0.048 mmol) in dry CH_2Cl_2 (2 mL) was cooled to 0 °C, and triethylamine (32 μL, 0.23 mmol) was added followed by tosylate chloride (18 mg, 0.09 mmol). The reaction mixture was stirred initially at 0 °C for 10 min and then at room temperature overnight. After quenching the reaction with cold water, the organic layer was separated. The aqueous layer was further extracted with CH_2Cl_2. The combined organic extracts were dried ($MgSO_4$) and concentrated, and the residue was purified by flash chromatography on silica eluted with hexane/EtOAc (80:20) to afford **17** as colorless oil (23 mg, 82%): ^{1}H NMR ($CDCl_3$, 400 MHz), δ 7.68 (d, *J* = 8.3 Hz, 2H), 7.23–7.34 (m, 7H), 6.96–7.03 (m, 2H), 6.75

(td, *J* = 0.9, 7.3 Hz, 1H), 6.56 (d, *J* = 8.3 Hz, 1H), 4.96 (d, *J* = 6.4 Hz, 1H), 4.33–4.39 (m, 1H), 4.24–4.30 (m, 1H), 3.87–3.90 (m, 1H), 3.79 (m, 1H), 3.69–3.74 (m, 1H), 3.48–3.55 (m, 2H), 3.03–3.08 (m, 2H), 2.87–2.92 (m, 1H), 2.59–2.64 (m, 1H), 2.40 (s, 3H), 1.39 (s, 9H). HRMS $[MH]^+$ Calcd for $C_{31}H_{38}NO_7S$: 568.2363, Found: 568.2362.

tert-Butyl (2*S*, 3*S*)-2-[α-(2-(3-methoxy-3-oxopropyl)phenoxy)(phenyl)methyl]morpholine-4-carboxylate (24)

To a mixture of **6** (45 mg, 0.15 mmol), methyl 3-(2-hydroxyphenyl)propionate (**22**) (54 mg, 0.3 mmol), and triphenylphosphine (80 mg, 0.3 mmol) in dry THF (3 mL) was added diisopropyl azodicarboxylate (60μL, 0.3 mmol) at 0 °C. The reaction mixture was allowed to reach room temperature and stirred during 48 h. The crude product was concentrated under reduced pressure and purified by flash chromatography on silica eluted with hexane/EtOAc (80:20) to afford **24** as colorless oil (38 mg, 55%): ^{1}H NMR ($CDCl_3$, 400 MHz), δ 7.25–7.37 (m, 5H), 7.10–7.13 (m, 1H), 6.96–7.00 (m, 1H), 6.77–6.84 (m, 1H), 6.63 (d, *J* = 8.0 Hz, 1H), 5.10 (d, *J* = 5.4 Hz, 1H), 3.91 (dd, *J* = 2.2, 11.4 Hz, 1H), 3.80–3.86 (m, 2H), 3.67 (s, 3H), 3.54 (td, *J* = 2.8, 11.7 Hz, 1H), 3.00–3.05 (m, 2H), 2.90 (t, *J* = 6.5 Hz, 2H), 2.74–2.78 (m, 1H), 2.71 (t, *J* = 6.4 Hz, 2H), 1.39 (s, 9H).

tert-Butyl (2*S*, 3*S*)-2-[α-(2-(3-hydroxypropyl)phenoxy)(phenyl)methyl]morpholine-4-carboxylate (26)

26 was prepared in 70% yield from **24** following the same procedure as described for **25**. ^{1}H NMR ($CDCl_3$, 400 MHz), δ 7.28–7.36 (m, 3H), 7.08–7.13 (m, 2H), 6.92–6.96 (m, 1H), 6.80–6.87 (m, 2H), 6.57 (d, *J* = 8.2 Hz, 1H), 5.12 (d, *J* = 5.1 Hz, 1H), 3.91–3.94 (m, 1H), 3.67–3.80 (m, 2H), 3.63 (t, *J* = 6.0 Hz, 2H), 3.52–3.60 (m, 1H), 2.82–3.00 (m, 3H), 2.77 (t, *J* = 6.4 Hz, 2H), 1.85–1.92 (m, 2H), 1.40 (s, 9H). HRMS $[MH]^+$ Calcd for $C_{25}H_{34}NO_5$: 428.2431, Found: 428.2430.

tert-Butyl (2*S*, 3*S*)-2-[α-(2-(3-tosyloxypropyl)phenoxy)(phenyl)methyl]morpholine-4-carboxylate (18)

18 was prepared in 55% yield from **26** following the same procedure as described for **17**. ^{1}H NMR ($CDCl_3$, 400 MHz), δ 7.79 (d, *J* = 8.6 Hz, 2H), 7.25–7.33 (m, 7H), 6.92–6.97 (m, 2H), 6.72 (t, *J* = 7.3 Hz, 1H), 6.61 (d, *J* =8.2 Hz, 1H), 5.05 (d, *J* = 6.0 Hz, 1H), 4.06 (t, *J* = 6.4 Hz, 2H), 3.74–3.94 (m, 4H), 3.48–3.54 (td, *J* = 2.7, 11.7 Hz, 2H), 2.85–2.95 (m, 1H), 2.71 (t, *J* = 7.3 Hz, 2H), 2.43 (s, 3H), 1.98–2.01 (m, 2H), 1.39 (s, 9H). HRMS $[MH]^+$ Calcd for $C_{32}H_{40}NO_7S$: 582.2520, Found: 582.2518.

Radiosynthesis. [^{11}C]1 and [^{11}C]4

No carrier-added $[^{11}C]CO_2$ was produced through the bombardment of $^{14}N_2$ gas containing 1% $^{16}O_2$ by a Siemens 11 MeV RDS 112 cyclitron at Emory University Hospital through the $^{14}N[p,\alpha]^{11}C$ reaction. A GE MicroLab methyl iodide system was employed for the conversion of $[^{11}C]CO_2$ to $[^{11}C]CH_3I$. The syntheses of [^{11}C]**1** and [^{11}C]**4** were performed using the trimethyltin precursors, **15** and **16**, respectively. A solution of $Pd_2(dba)_3$ (1.5 mg, 1.6 μmol) and (*o*-Tol)$_3$P (2.0 mg, 6.4 μmol) in DMF (0.35 mL) was prepared in a 1 mL sealed conical vial and purged with Ar gas for 15 min. $^{11}CH_3I$ was bubbled through the solution at 0 °C and then the reaction mixture was left standing at room temperature for 4 min after which it was transferred to a 3 mL dry, Ar purged and sealed conical vial containing the tin precursor (2 mg), CuCl (2.0 mg, 20 μmol) and K_2CO_3 (2.0 mg, 14.5 μmol) dissolved in DMF (0.1 mL). The vial was shaken vigorously before heating at 100 °C for 5 min, TFA (0.22 mL, ~750 equiv) was added, and the solution was heated at 100 °C for 7 min, cooled to 0 °C, and neutralized by addition of 5 M NH_4OH(aq) (0.6 mL,~800 equiv). The reaction mixture was filtered and then purified by semipreparative HPLC (Water XTerra Prep RP_{18} 5μm, 19 × 100 mm) at a 9

mL/min flow rate. The retention time of [^{11}C]**1** was 11 min with buffered mobile phase consisting 57:43:0.1 v/v/v MeOH/H_2O/Et_3N. The retention time of [^{11}C]**4** was 14 min with buffered mobile phase consisting 58:42:0.1 v/v/v MeOH/H_2O/Et_3N. The desired fractions were combined, diluted with double volume of water and loaded onto a Waters C_{18} SepPak cartridge that was washed with saline (0.9% NaCl, 40 mL) and ethanol (0.5 mL). The radioactive product was washed out of the cartridge by absolute ethanol (1.5 mL) into a sealed sterile vial containing 3.5 mL of saline. The resulting solution was transferred under argon pressure through a Millipore filter (pore size 1.0 μm) followed by a smaller one (pore size 0.2 μm), to a 30 mL sterile vial containing 10 mL of saline and is ready for PET study. The total synthesis time (including purification and formulation) of [^{11}C]**1** and [^{11}C]**4** labeling was approximately 60 min from the end of bombardment. The final product was analyzed on an analytical HPLC (Waters Nova-Pak C_{18} 3.9×150 mm) eluted with MeOH/H_2O/Et_3N = 70:30:0.1 at 1.0 mL/min (t_R = 4.3 min for [^{11}C]**1** and 6.7 min for [^{11}C]**4**). Radioactivity and absorbance (254 nm) were monitored to confirm the radiochemical purity and measure the specific activity.

[^{18}F]2 and [^{18}F]3

No-carrier-added (NCA) [^{18}F]-fluoride was produced at Emory University Hospital with a 11MeV Siemens RDS 112 negative-ion cyclotron (Knoxville, TN, USA) by the ^{18}O (p, n) ^{18}F reaction using [^{18}O] enriched water (>95 atom%). The radiosyntheses of [^{18}F]**2** and [^{18}F]**3** were performed in a chemical process control unit (CPCU) obtained from CTI, Inc. (Knoxville, TN, USA). NCA aqueous [^{18}F]-fluoride (0.8 mL) delivered to the trap/release cartridge (DW-TRC, D&W, Inc.) was released with 0.6 mL of water containing 0.9 mg of potassium carbonate as K[^{18}F]F and added to a Pyrex vessel which contained 5 mg of Kryptofix 2.2.2 in 1 mL of CH_3CN. The water was evaporated using a stream of nitrogen at 110 °C and co-evaporated to dryness with CH_3CN (3 mL). The tosylate precursor **17** or **18** (2 mg in 1 mL of AcCN) was then added to the dried K[^{18}F]F and the solution was heated at 90 °C for 10 min and then cooled to room temperature. Ether (3×3 mL) was added and the contents of the vessel were transferred through the silica SepPak to a V-vial. After evaporation of ether, 6 M HCl (0.21 mL) was added to the residue, and the solution was heated at 100 °C for 7 min, cooled to 0 °C, and neutralized by addition of 6 M NH_4OH (0.22 mL). The solution was purified by semipreparative HPLC (Water XTerra Prep RP_{18} 5μm, 19 × 100 mm). The retention time of [^{18}F]**2** was t_R (range) = 23–26 min with mobile phase consisting 52:48:0.1 v/v/v MeOH/H_2O/Et_3N at a 6 mL/min flow rate. The retention time of [^{18}F]**3** was t_R (range) = 26–29 min with mobile phase consisting 52:48:0.1 v/v/v MeOH/H_2O/Et_3N at a 8 mL/min flow rate. The dose formulation was conducted by the same procedure described above as for [^{11}C]**1**. The total synthesis time was 100 min from EOB with 6–11% radiochemical yield for both compounds (decay-corrected from [^{18}F]F^-). The radiochemical purities of radioligands were determined by an analytical radio-HPLC (waters Nova-Pak C_{18} 3.9 × 150 mm) using a UV detector and a radioactivity detector with or without coinjection with unlabeled reference compounds. The specific activities were determined by the UV absorbance of the radioactive peaks as compared with standard curves of unlabeled reference compounds. The retention time of [^{18}F]**2** and [^{18}F]**3** was 4.0 and 5.7 min, respectively, on analytical HPLC eluted with 70:30:0.1 v/v/v MeOH/H_2O/Et_3N at a 1 mL/min flow rate.

Lipophilicity Measurements

Measurement of distribution coefficients of radiolabeled compounds were performed according to a previously reported procedure.[42] Briefly, The test tubes containing 2 mL of 1-octanol, 2 mL of 0.02 M sodium phosphate buffer (pH = 7.4) and ~5–10 μCi portion of the radiotracer were vortexed for 10 min at room temperature and then centrifuged for 5 min. Samples (0.5 mL) from the 1-octanol and buffer layers were counted in a Packard Cobra II automated gamma-counter and decay corrected. The measurement was repeated three times. The log $P_{7.4}$ values were calculated for each replicate with the following equation: log $P_{7.4}$ =

log [(counts in octanol phase)/(counts in buffer phase)]. The log $P_{7.4}$ measurements from each replication were averaged to give the log $P_{7.4}$ values for the radiotracer.

MicroPET Studies in Anesthetized Monkeys

MicroPET studies were performed in anesthetized adult male rhesus monkeys using a Concorde microPET P4 system (Knoxville, TN) according to a previously reported procedure.[45] The MicroPET imaging studies were performed using 15–20 mCi of [^{11}C]**1** or [^{11}C]**4**, or 4–5 mCi of [^{18}F]**2** or [^{18}F]**3** with and without injection of pharmacological doses of monoamine transporter ligands. Emission data were collected in the microPET imaging studies continuously for 125 min after injection of [^{11}C]**1** or [^{11}C]**4** or 240 min after injection of [^{18}F]**2** or [^{18}F]**3** and then binned for analysis. For generation of time-activity curves, regions of interest (ROIs) were drawn manually based on the anatomical landmarks visible in reconstructed PET images using ASIPro software (Concorde, Knoxville, TN). The data were converted to standard uptake values (SUV). SUV values were defined as [the pixel value in (μCi/mL) × weight of animal (mg)]/[dose (μCi)].

PET Studies in Awake Monkeys

PET studies were performed in awake rhesus monkeys. The subjects received extensive behavioral training to ensure immobility throughout the neuroimaging session as described in a previous publication.[48] Quantitative brain PET imaging were acquired using an ECAT 921 EXACT scanner (Siemens/CTI). The PET imagings for each subject were coregistered with MRI. The data were converted to standard uptake values (SUV).

Supplementary Material

Refer to Web version on PubMed Central for supplementary material.

Acknowledgment

We thank Larry Williams for his contribution in the microPET studies and Anthony M. Giamis and Eugene Malveaux for their contributions in the rodent tissue distribution studies. The authors are supported by NIH 1-R21-MH-66622-01, MH-42088, RR-000039, MH-39415, and MH-52899. We acknowledge the use of Shared Instrumentation provided by grants from the National Institutes of Health and National Science Foundation.

References

1. Blakely RD, DeFelice LJ, Hartzell HC. Molecular Physiology of Norepinephrine and Serotonin Transporter. J. Exp. Biol 1994;196:263–281. [PubMed: 7823027]
2. Pacholcyzk T, Blakely RD, Amara SG. Express Cloning of a Cocaine and Antidepressant-sensitive Human Noradrenaline Transporter. Nature 1991;350:350–354. [PubMed: 2008212]
3. Ordway GA, Stockmeyer CA, Mason GW, Klimek V. Pharmacology and Distribution of Norepinephrine Transporters in the Human Locus Coeruleus and Raphe Nuclei. J. Neuroscience 1997;17:1710–1719.
4. Tejani-Butt SM. [^{3}H]Nisoxetine: A Radioligand for Quantitation of Norepinephrine Uptake Sites by Autoradiography or by Homogenate Binding. J. Phar. Exp. Ther 1992;260:427–436.
5. Gross-Isseroff R, Israeli M, Biegon A. Autoradiographic Analysis of [^{3}H]Desmethylimipramine Binding in the Human Brain Postmortem. Brain Res 1988;456:120–126. [PubMed: 3409030]
6. Ressler KJ, Nemeroff CB. Role of norepinephrine in the pathophysiology and treatment of mood disorders. Biol. Psychiatry 1999;46:1219–1233. [PubMed: 10560027]
7. Tejani-Butt SM, Yang J, Zaffar H. Norepinephrine transporter sites are decreased in the locus coeruleus in Alzheimer's disease. Brain Res 1993;631:147–150. [PubMed: 8298987]

8. Gesi M, Soldani P, Giorgi FS, Santinami A, Bonaccorsi I, Fornai F. The role of the locus coeruleus in the development of Parkinson's disease. Neurosci. Biobehav. Rev 2000;24:655–668. [PubMed: 10940440]
9. Biederman J, Spencer T. Attention-deficit/hyperactivity disorder (ADHD) as a noradrenergic disorder. Biol. Psych 1999;46:1234–1242.
10. Schou M, Sovago J, Pike VW, Gulyas B, Bogeso KP, Farde L, Halldin C. Synthesis and positron emission tomography evaluation of three norepinephrine transporter radioligands: [C-11] desipramine, [C-11]talopram and [C-11]talsupram. Mol. Imaging Biol 2006;8:1–8. [PubMed: 16322935]
11. Van Dort ME, Kim JH, Tluczek L, Wieland DM. Synthesis of ^{11}C-labeled desipramine and its metabolite 2-hydroxydesipramine: potential radiotracers for PET studies of the norepinephrine transporter. Nucl. Med. Biol 1997;24:707–711. [PubMed: 9428594]
12. Schou M, Pike VW, Sovago J, Gulyas B, Gallagher PT, Dobson DR, Walter MW, Rudyk H, Farde L, Halldin C. Synthesis of ^{11}C-labelled (R)-OHDMI and CFMME and their evaluation as candidate radioligands for imaging central norepinephrine transporters with PET. Bioorg. Med. Chem 2007;15:616–625. [PubMed: 17123820]
13. Ding Y-S, Lin K-S, Logan J, Benveniste H, Carter P. Comparative evaluation of positron emission tomography radiotracers for imaging the norepinephrine transporter: (*S*,*S*) and (*R*,*R*) enatiomers of reboxetine analogs ([^{11}C]methylreboxetine, 3-Cl-[^{11}C]methylreboxetine and [^{18}F]fluroreboxetine), (*R*)-[^{11}C]nisoxetine, [^{11}C]oxaprotiline and [^{11}C]lortalamine. J. Neurochem 2005;94:337–351. [PubMed: 15998285]
14. Kung M-P, Choi S-R, Hou C, Zhuang Z-P, Foulon C, Kung HF. Selective binding of 2-[^{125}I]iodo-nisoxetine to norepinephrine transporters in the brain. Nucl. Med. Biol 2004;31:533–541. [PubMed: 15219270]
15. Lakshmi B, Kung M-P, Lieberman B, Zhao J, Waterhouse R, Kung HF. (*R*)-N-Methyl-3-(3-^{125}I-pyridin-2-yloxy)-3-phenylpropan-1-amine: a novel probe for norepinephrine transporters. Nucl. Med. Biol 2008;35:43–52. [PubMed: 18158942]
16. Schou M, Pike VW, Varrone A, Gulyas B, Farde L, Halldin C. Synthesis and PET evaluation of (*R*)-[*S*-methyl-^{11}C]thionisoxetine, a candidate radioligand for imaging brain norepinephrine transporters. J. Labelled Compd. Radiopharm 2006;49:1007–1019.
17. McConathy J, Owens MJ, Kilts CD, Malveaux EJ, Camp VM, Votaw JR, Nemeroff CB, Goodman MM. Synthesis and biological evaluation of [^{11}C]talopram and [^{11}C]talsupram: candidate PET ligands for the norepineprine transporter. Nucl. Med. Biol 2004;31:705–718. [PubMed: 15246361]
18. Ding Y-S, Lin KS, Gaza V, Carter P, Alexoff D, Logan J, et al. Evaluation of a New Norepinephrine Transporter PET Ligand in Baboons, both Brain and Peripheral Organ. Synapse 2003;50:345–352. [PubMed: 14556239]
19. Wilson AA, Johnson DP, Mozley D, Hussey D, Ginovart N, Nobrega J, Garcia A, Meyer J, Houls S. Synthesis and in vivo Evaluation of Novel Radiotracers for the in vivo Imaging of the Norepinephrine Transporter. Nucl. Med. Biol 2003;30:85–92. [PubMed: 12623106]
20. Schou M, Halldin C, Sovago J, Pike VW, Gulyas B, Mozley PD, Johnson DP, Hall H, Innis RB, Farde L. Specific *in vivo* binding to the norepinephrine transporter demonstrated with the PET radioligand, (*S*,*S*)-[^{11}C]MeNER. Nucl. Med. Biol 2003;30:707–714. [PubMed: 14499328]
21. Schou M, Halldin C, Sovago J, Pike VW, Hall H, Gulyas B, Mozley PD, Dobson D, Shchukin E, Innis RB, Farde L. PET Evaluation of Novel Radiofluorinated Reboxetine Analogs as Norepinephrine Transporter Probes in the Monkey Brain. Synapse 2004;53:57–67. [PubMed: 15170818]
22. Seneca N, Gulyas B, Varrone A, Schou M, Airaksinen A, Tauscher J, Vandenhende F, Kielbasa W, Farde L, Innis RB, Halldin C. Atomoxetine occupies the norepinephrine transporter in a dose-dependent fashion: a PET study in nonhuman primate brain using (*S*,*S*)-[^{18}F]FMeNER-D_2. Psychopharmacology 2006;188:119–127. [PubMed: 16896954]
23. Kanegawa N, Kiyono Y, Kimura H, Sugita T, Kajiyama S, Kawashima H, Ueda M, Kuge Y, Saji H. Synthesis and evaluation of radioiodinated (S,S)-2-(α-(2-iodophenoxy)benzyl)morpholine for imaging brain norepinephrine transporter. Eur. J. Nucl. Med. Mol. Imaging 2006;33:639–647. [PubMed: 16523308]

24. Tamagnan GD, Brenner E, Alagille D, Staley JK, Haile C, Koren A, Early M, Baldwin RM, Tarazi FI, Baldessarini RJ, Jarkas N, Goodman MM, Seibyl JP. Development of SPECT imaging agents for the norepinephrine transporters: [^{123}I]INER. Bioorg. Med. Chem. Lett 2007;17:533–537. [PubMed: 17095215]
25. Lin K-S, Ding Y-S, Kim S-W, Kil K-E. Synthesis, enantiomeric resolution, F-18 labeling and biodistribution of reboxetine analogs: promising radioligands for imaging the norepinephrine transporter with positron emission tomography. Nucl. Med. Biol 2005;32:415–422. [PubMed: 15878511]
26. Severance A, Milak MS, Kumar JSD, Prabhakaran J, Majo VJ, Simpson NR, Van Heertum RL, Arango V, Mann JJ, Parsey RV. In vivo assessment of [^{11}C]MRB as a prospective PET ligand for imaging the norepinephrine transporter. Eur. J. Nucl. Med. Mol. Imaging 2007;34:688–693. [PubMed: 17180600]
27. Logan J, Wang G-J, Telang F, Fowler JS, Alexoff D, Zabroski J, Jayne M, Hubbard B, King P, Carter P, Shea C, Xu Y, Muench L, Schlyer D, Learned-Coughlin S, Cosson V, Volkow ND, Ding Y-S. Imaging the norepinephrine transporter in humans with (*S*,*S*)-[^{11}C]*O*-methyl reboxetine and PET: problems and progress. Nucl. Med. Biol 2007;34:667–679. [PubMed: 17707807]
28. Takano A, Gulyas B, Varrone A, Karlsson P, Schou M, Airaksinen AJ, Vandenhende F, Tauscher J, Halldin C. Imaging the norepinephrine transporter with position emission tomography: initial human studies with (*S*,*S*)-[^{18}F]FMeNER-D$_2$. Eur. J. Nucl. Med. Mol. Imaging 2008;35:153–157. [PubMed: 17909794]
29. Boot J, Cases M, Clark BP, Findlay J, Gallagher PT, Hayhurst L, Man Teresa, Montalbetti C, Rathmell RE, Rudyk H, Walter MW, Whatton M, Wood V. Discovery and structure-activity relationships of novel selective norepinephrine and dual serotonin/norepinephrine reuptake inhibitors. Bioorg. Med. Chem. Lett 2005;15:699–703. [PubMed: 15664840]
30. Zeng F, Jarkas N, Stehouwer JS, Voll RJ, Owens MJ, Kilts CD, Nemeroff CB, Goodman MM. Synthesis, in vitro characterization, and radiolabeling of reboxetine analogs as potential PET radioligands for imaging the norepinephrine transporter. Bioorg. Med. Chem 2008;16:783–793. [PubMed: 17983754]
31. Brenner E, Baldwin RM, Tamagnan G. Asymmetric Synthesis of (+)-(*S*,*S*)-Reboxetine via a New (*S*)-2-(Hydroxymethyl)morpholine Preparation. Org. Lett 2005;7:937–939. [PubMed: 15727479]
32. Rose-Munch F, Rose E, Semra A, Mignon L, Garcia-Oricain J. Substitutions nucleophiles aromatiques S_NAr de fluorobenzenetricarbonylchrome. J. Organometallic chem 1989;363:297–309.
33. Lee KC, Moon BS, Lee JH, Chung K-H, Katzenellenbogen JA, Chi DY. Synthesis and Binding Affinities of Fluoroalkylated Raloxifenes. Bioorg. Med. Chem 2003;11:3649–3658. [PubMed: 12901910]
34. Figuly GD, Loop CK, Martin JC. Directed Ortho-Lithiation of Lithium Thiophenolate. New Methodology for the Preparation of Ortho-Substituted Thiophenols and Related Compounds. J. Am. Chem. Soc 1989;111:654–658.
35. Van Dort PC, Fuchs PL. Sulfones as Radical Progenitors: An Unprecedented Example of Homolytic Sulfone Cleavage Facilitated by *o*-Stannyl Substitution of Aryl Sulfones. J. Org. Chem 1997;62:7137–7141. [PubMed: 11671817]
36. Björkman M, Doi H, Resul B, Suzuki M, Noyori R, Watanable Y, Långstrom B. SYNTHESIS OF A ^{11}C-LABELLED PROSTAGLANDIN $F_{2\alpha}$ANALOGUE USING AN IMPROVED METHOD FOR STILLE REACTIONS WITH [^{11}C]METHYL IODIDE. J. Labelled Cpd. Radiopharm 2000;43:1327–1334.
37. Björkman M, Andersson Y, Doi H, Kato K, Suzuki M, Noyori R, Watanable Y, Långstrom B. Synthesis of ^{11}C/^{13}C-labelled prostacyclins. Acta Chem. Scand 1998;52:635–640. [PubMed: 9586195]
38. Yu M, Någren K, Halldin C, Swahn C-G, Helfenbein J, Guilloteau D. Synthesis of [*P-methyl*^{11}C] RTI-32: A new tool for the in vivo evaluation of the metabolism of phenyltropane dopamine reuptake compounds. J. Labelled Compd. Radiopharm 1999;42:S469–S471.
39. Sandell J, Halldin C, Sovago J, Chou Y-H, Gulyas B, Yu M, Emond P, Nagren K, Guilloteau D, Farde L. PET examination of [^{11}C]5-methyl-6-nitroquipazine, a radioligand for visualization of the serotonin transporter. Nucl. Med. Biol 2002;29:651–656. [PubMed: 12234589]

40. Suzuki M, Doi H, Björkman M, Andersson Y, Langstrom B, Watanabe Y, Noyori R. Rapid Coupling of Methyl Iodide with Aryltributylstannanes Mediated by Palladium(0) Complexes: A General Protocol for the Synthesis of $^{11}CH_3$-Labeled PET Tracers. Chem. Eur. J 1997;3:2039–2042.
41. Lemaire C, Plenevaux A, Aerts J, Del Fiore G, Brihaye C, Le Bars D, Comar D, Luxen A. Solid-Phase ExtractionAn Alternative to the Use of Rotary Evaporators for Solvent Removal in the rapid Formulation of PET Radiopharmaceuticals. J. Labelled Compd. Radiopharm 1999;42:63–75.
42. Wilson AA, Houle S. Radiosynthesis of Carbon-11 Labeled *N*-Methyl-2-(arylthio)benzylamines: Potential Radiotracers for the Serotonin Reuptake Receptor. J. Labelled Compd. Radiopharm 1999;42:1277–1288.
43. Dischino DD, Welch MJ, Kilbourn MR, Raichle ME. Relationship between Lipophilicity and Brain Extraction of C-11-Labeled Radiopharmaceuticals. J. Nucl. Med 1983;24:1030–1038. [PubMed: 6605416]
44. Owens MJ, Morgan WN, Plott SJ, Nemeroff CB. Neurotransmitter Receptor and Transporter Binding Profile of Antidepressants and Their Metabolites. J. Pharmacol. Exp. Ther 1997;283:1305–1322. [PubMed: 9400006]
45. Plisson C, McConathy J, Martarello L, Malveaux EJ, Camp VM, Williams L, Votaw JR, Goodman MM. Synthesis, Radiosynthesis, and Biological Evaluation of Carbon-11 and Iodine-123 Labeled 2 β-Carbomethoxy-3β-[4'-((Z)-2-haloethenyl)phenyl]tropanes: Candidate Radioligands for in Vivo Imaging of the Serotonin Transporter. J. Med. Chem 2004;47:1122–1135. [PubMed: 14971892]
46. The binding affinities of the racemic mixture of compound **4** containing (S,S) and (R,R) enantiomers were determined through reuptake inhibition binding assays in rat transporters and reported in Ref. 29.
47. Votaw JR, Byas-Smith MG, Voll R, Halkar R, Goodman MM. Isoflurance Alters the Amount of Dopamine Transporter Expressed on the Plasma Membrane in Human. Anesthesiology 2004;101:1128–1135. [PubMed: 15505448]
48. Howell LL, Hoffman JM, Votaw JR, Landrum AM, Jordan JF. An apparatus and behavioral training protocol to conduct positron emission tomography (PET) neuroimaging in conscious rhesus monkeys. J. Neuroscience Methods 2001;106:161–169.

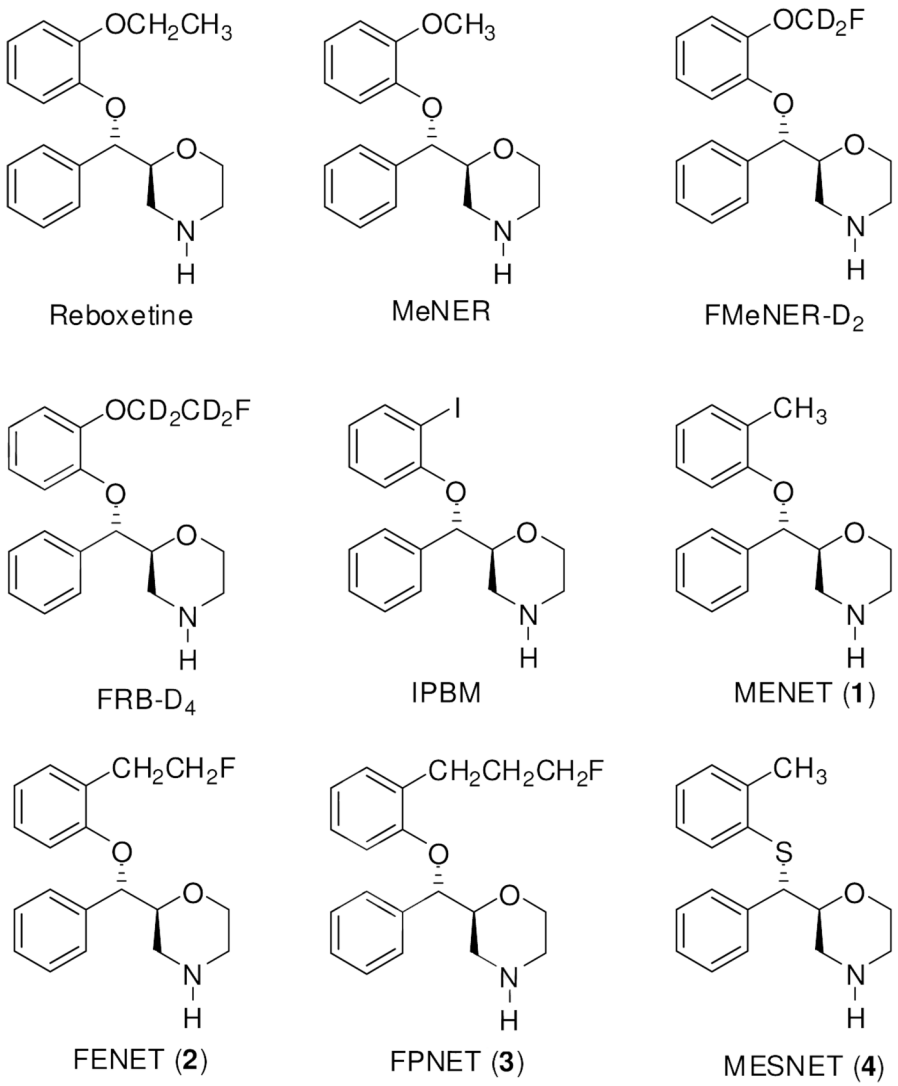

Figure 1.
(2*S*, 3*S*) Enantiomer of reboxetine derivatives.

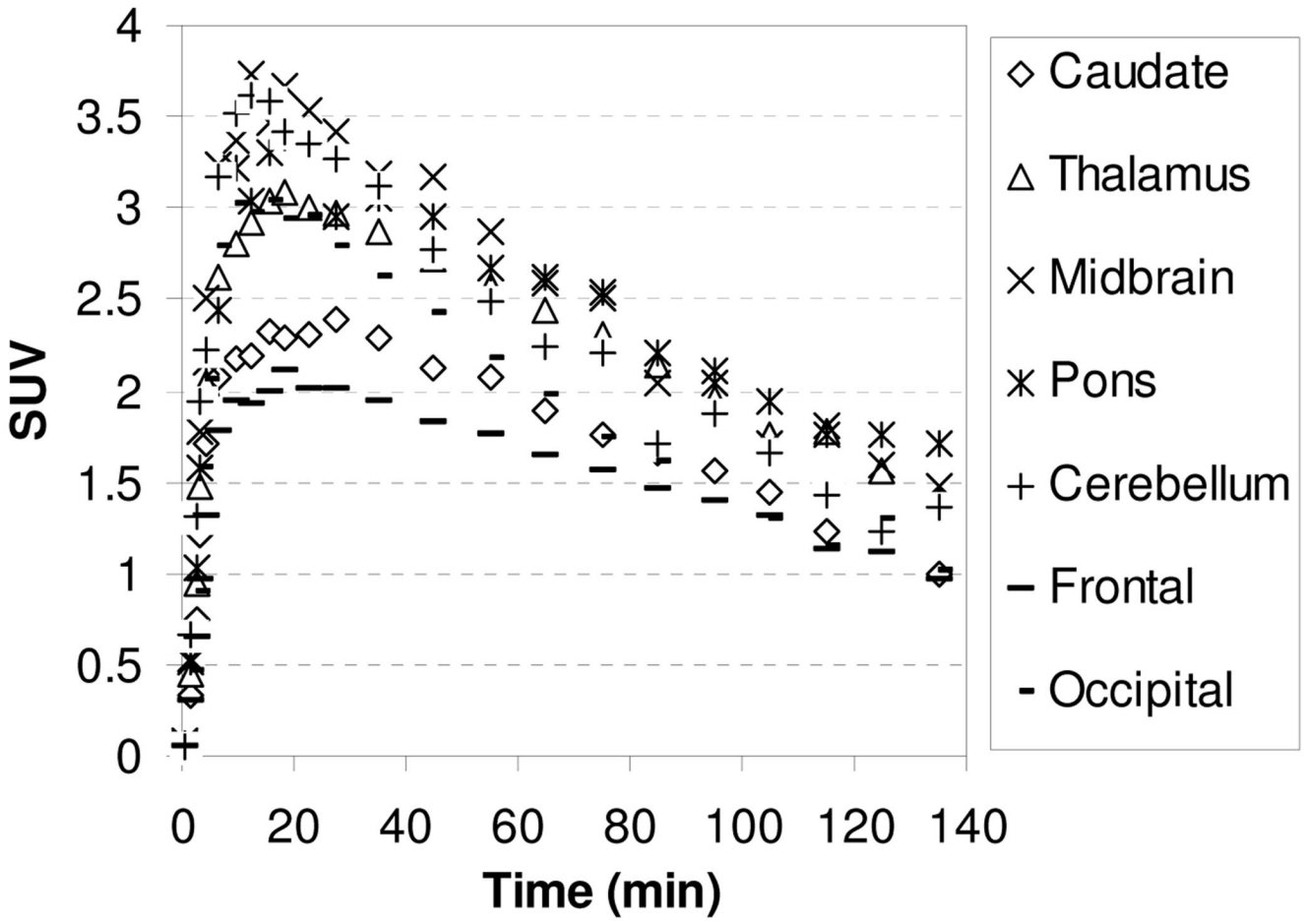

Figure 2.
MicroPET baseline study TACs for the brain regions of a rhesus monkey after injection of [^{11}C]**1**.

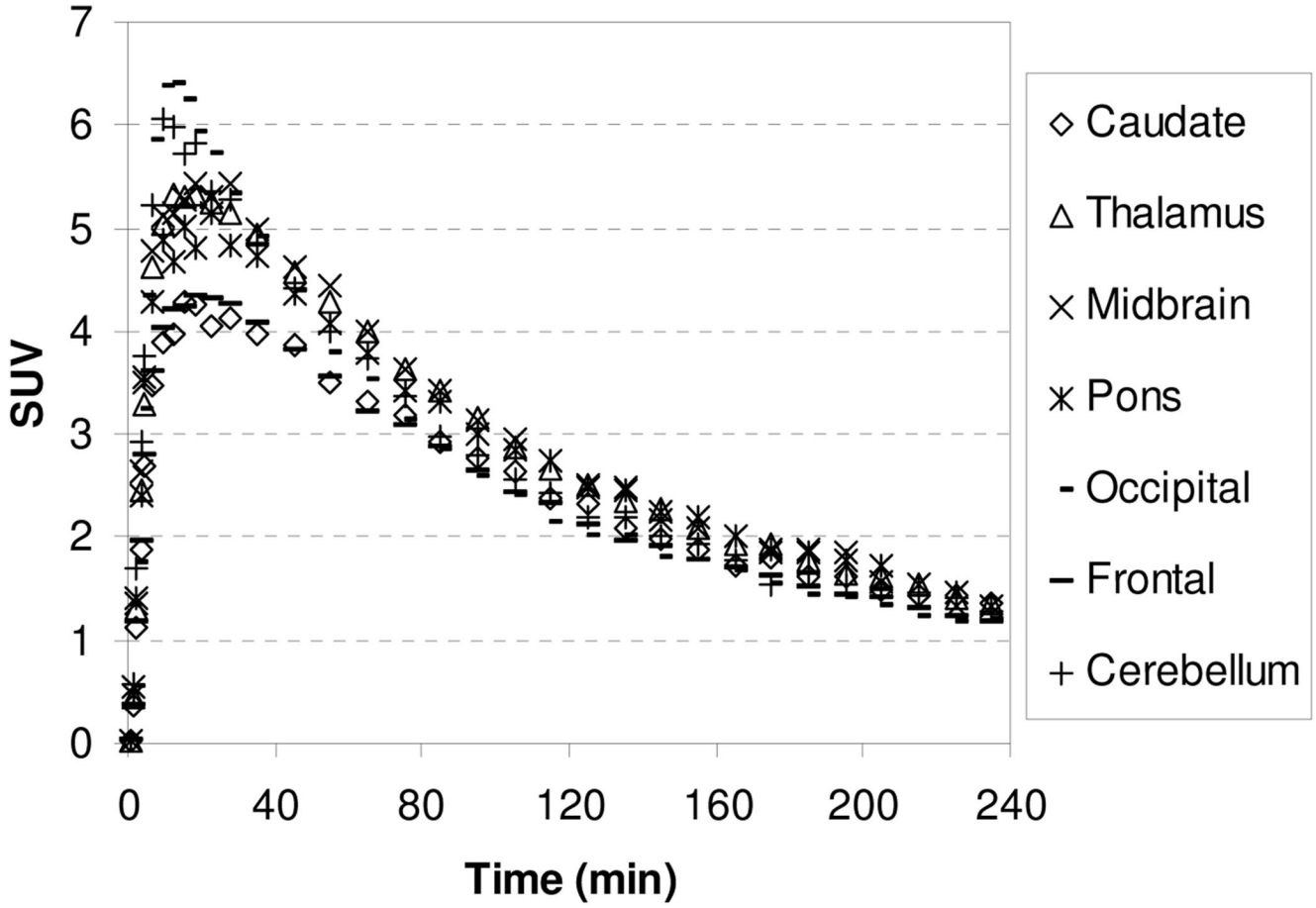

Figure 3.
MicroPET baseline study TACs for the brain regions of a rhesus monkey after injection of [^{18}F]**2**.

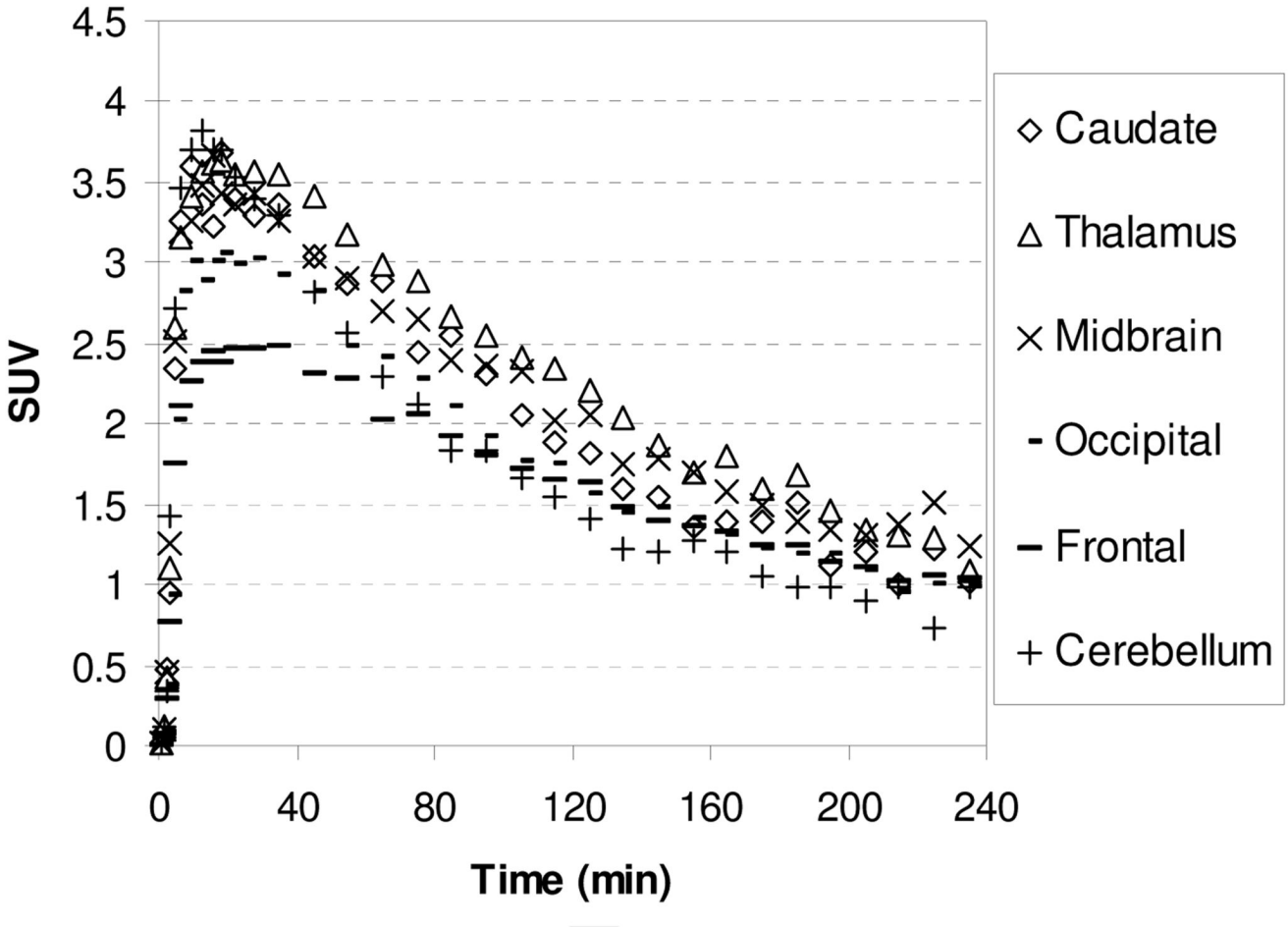

Figure 4.
MicroPET baseline study TACs for the brain regions of a rhesus monkey after injection of [^{18}F]**3**.

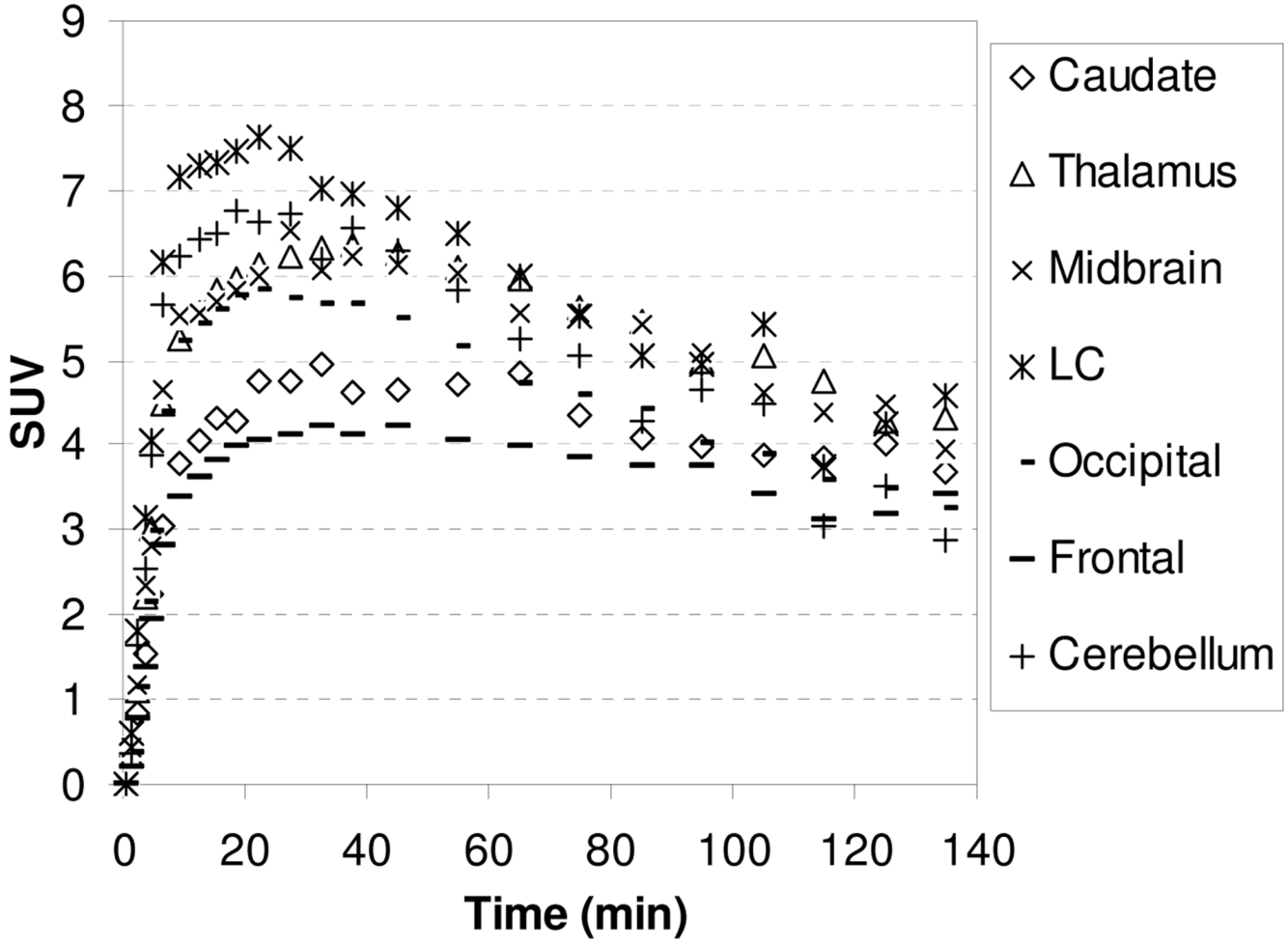

Figure 5.
MicroPET baseline study TACs for the brain regions of a rhesus monkey after injection of [^{11}C]**4**.

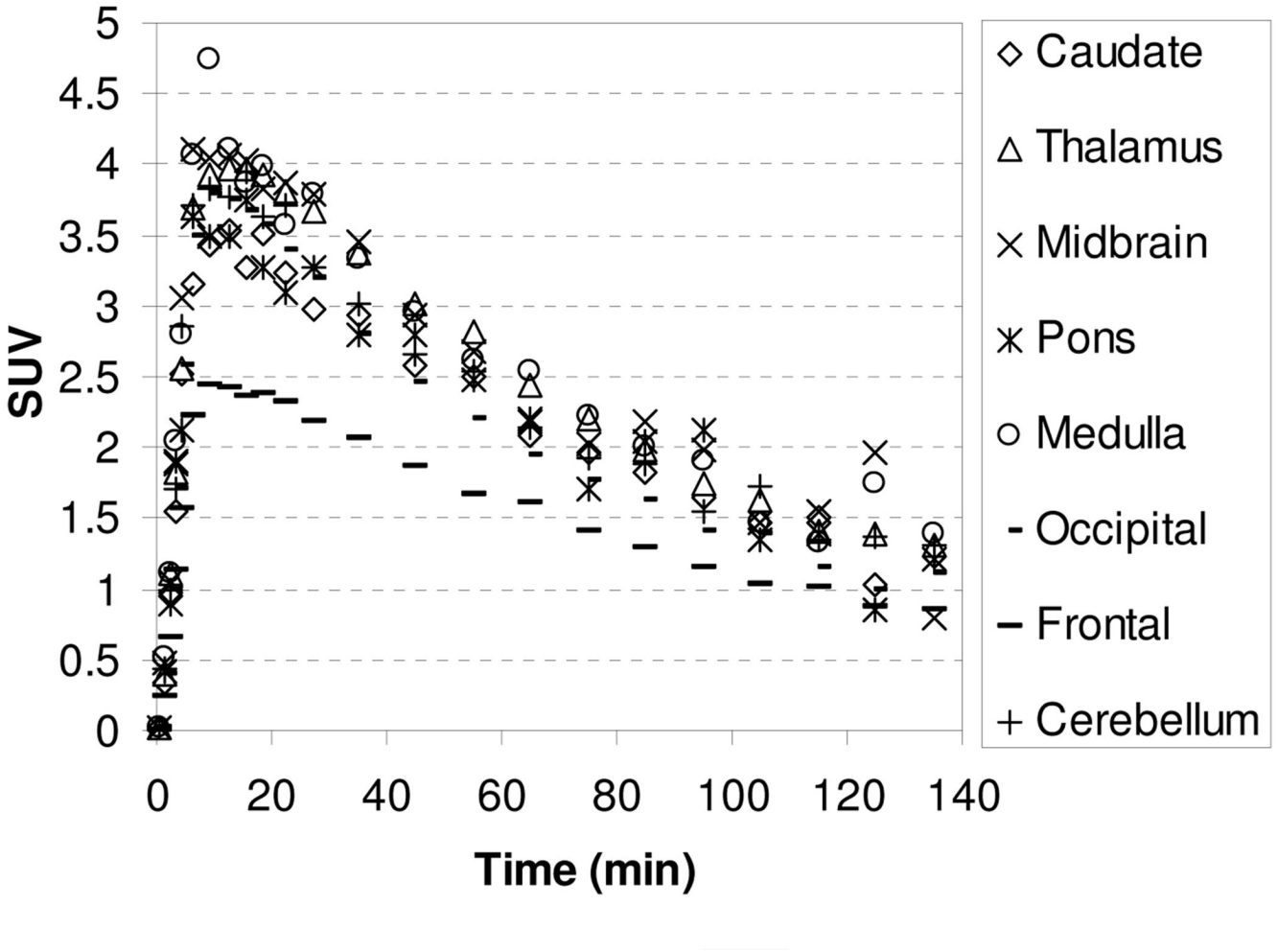

Figure 6.
Time-activity curves for brain regions for [^{11}C]**1** after desipramine (0.125 mg/kg) pretreatment.

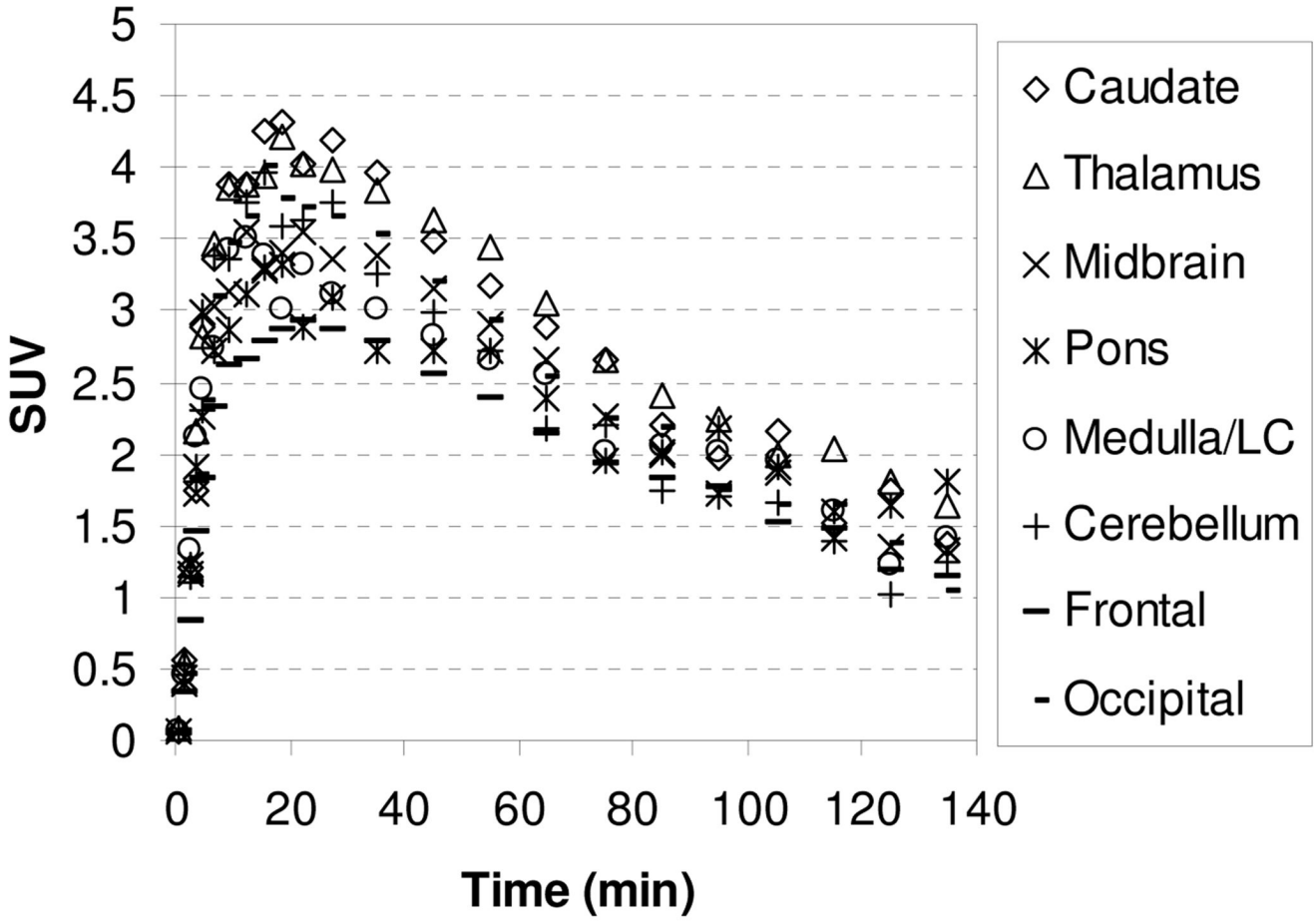

Figure 7.
Time-activity curves for brain regions for [^{11}C]**1** after desipramine (0.25 mg/kg) pretreatment.

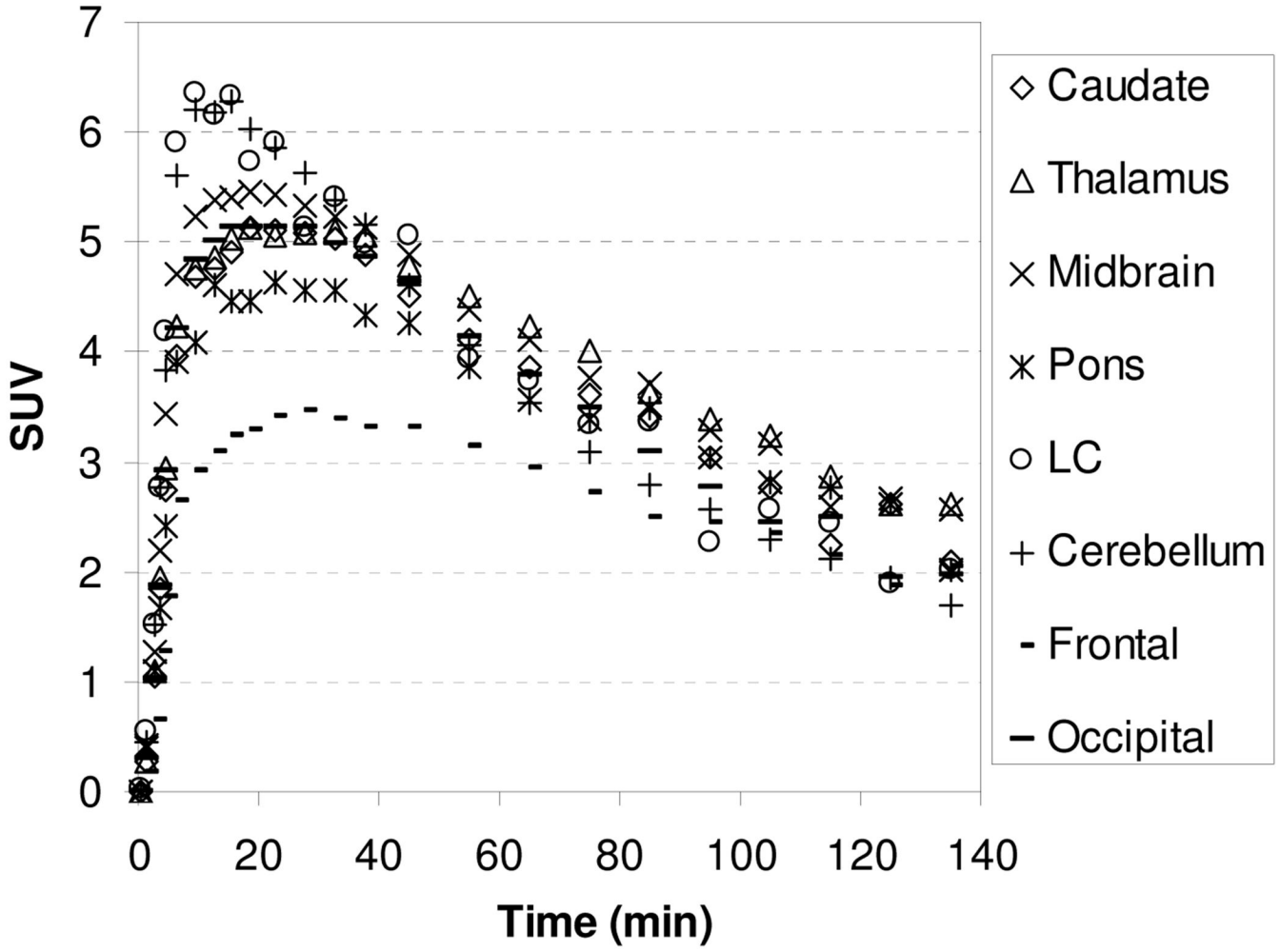

Figure 8.
Time-activity curves for brain regions for [^{11}C]**4** after desipramine (0.125 mg/kg) pretreatment.

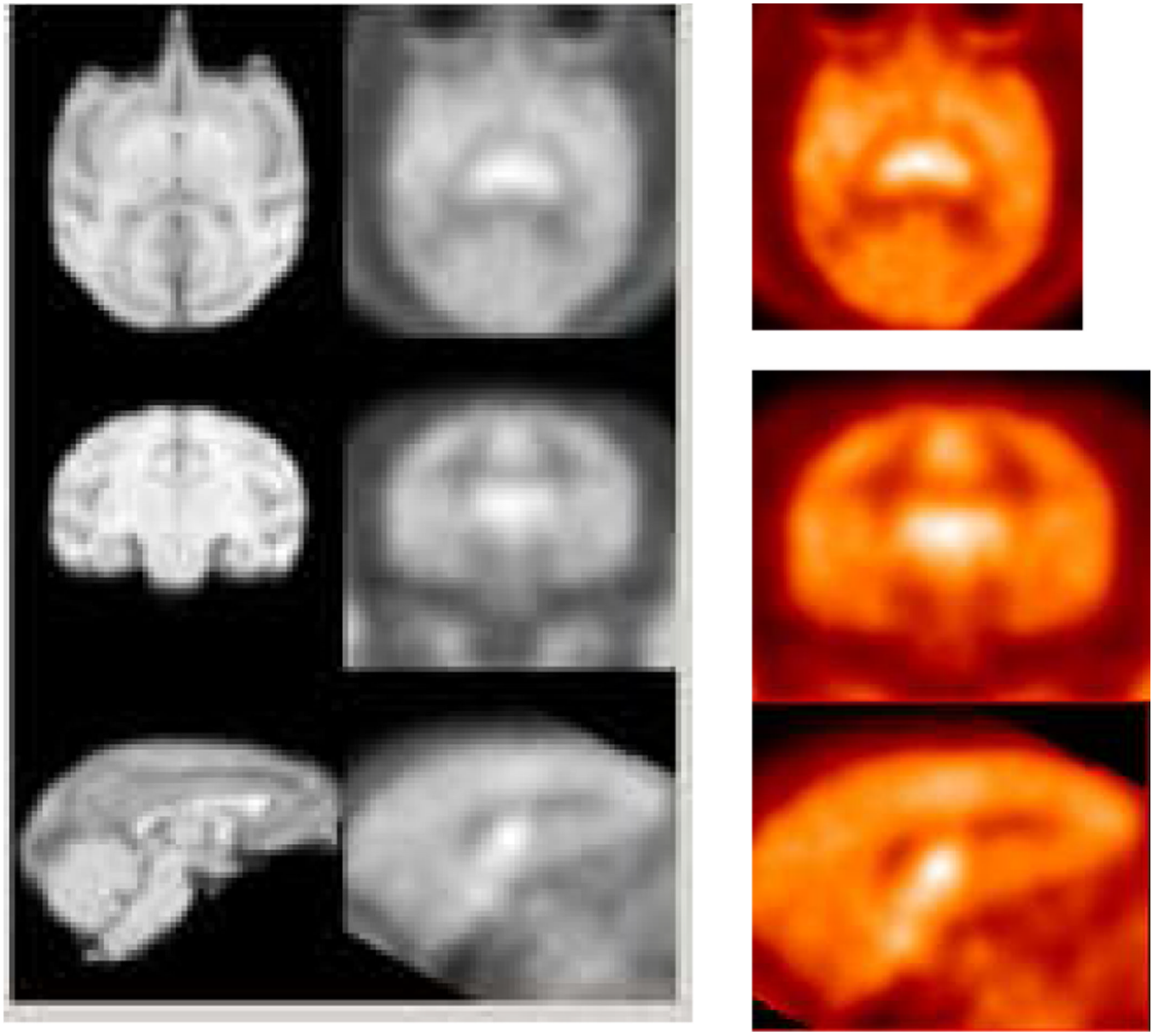

Figure 9.
HRRT PET images (right and center) obtained by injection of [^{11}C]**1** into an awake rhesus monkey and coregistered with MRI.

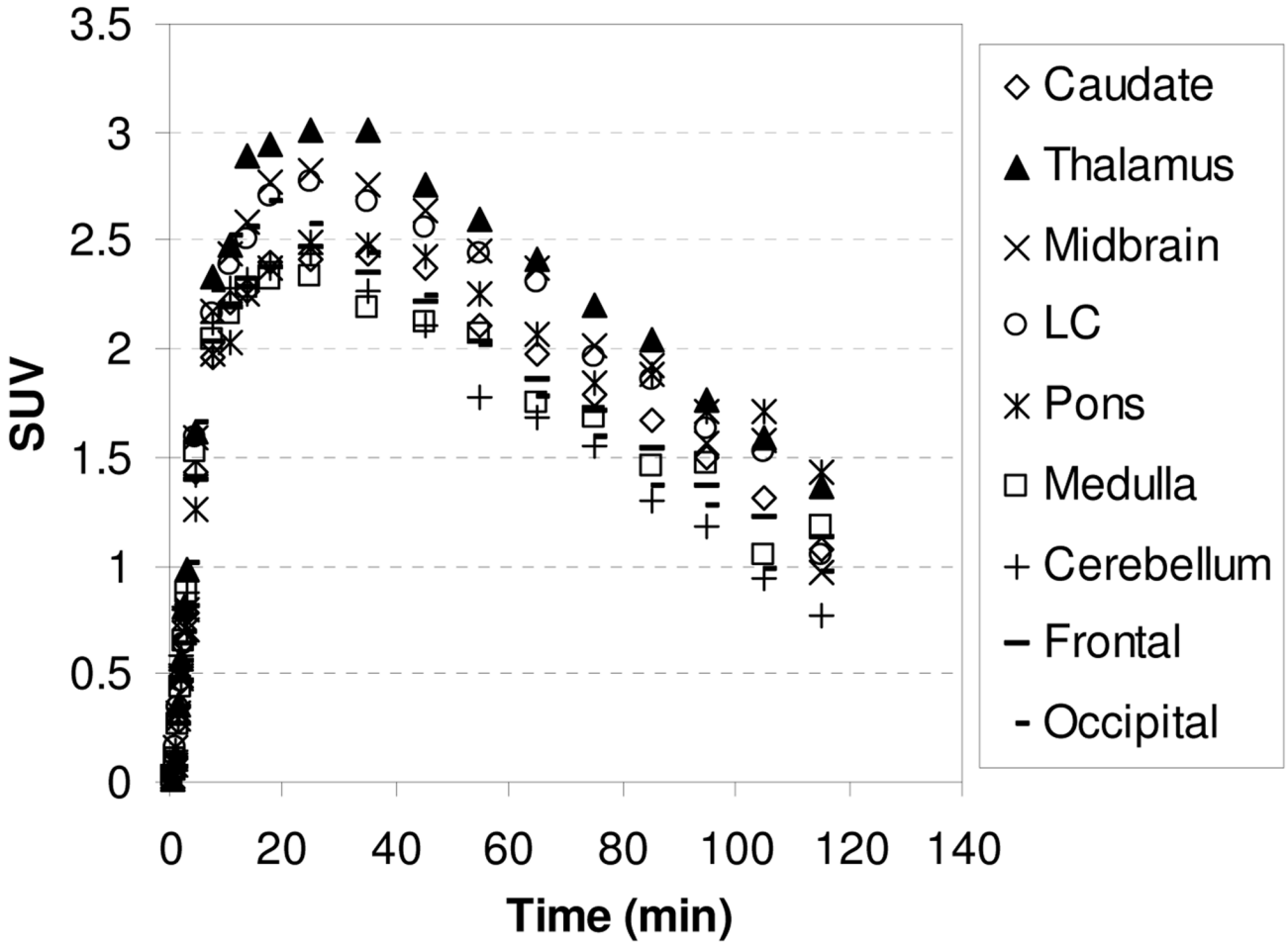

Figure 10.
HRRT TACs obtained after injection of [^{11}C]**1** into an awake rhesus monkey.

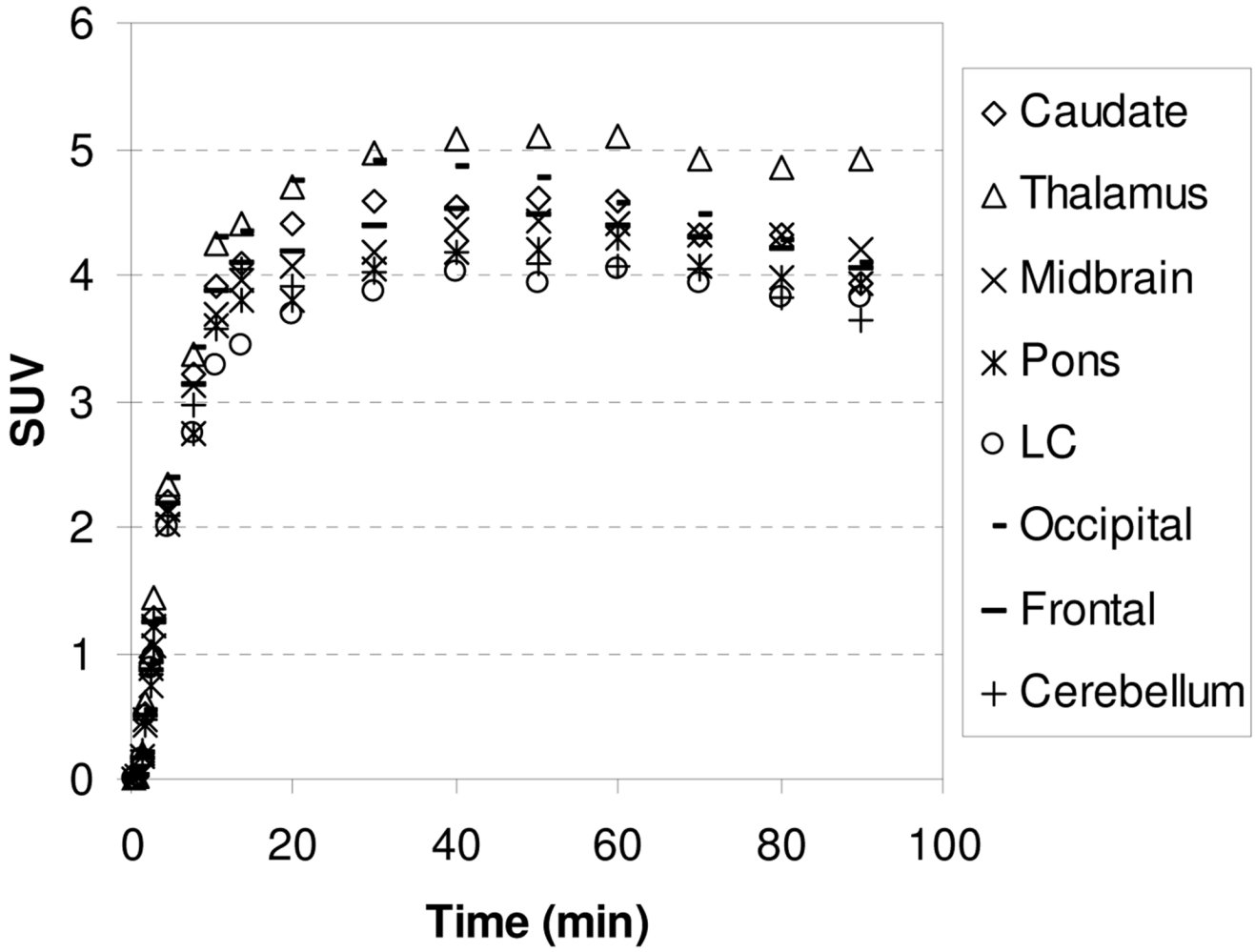

Figure 11.
HRRT TACs obtained after injection of [^{11}C]**4** into an awake rhesus monkey.

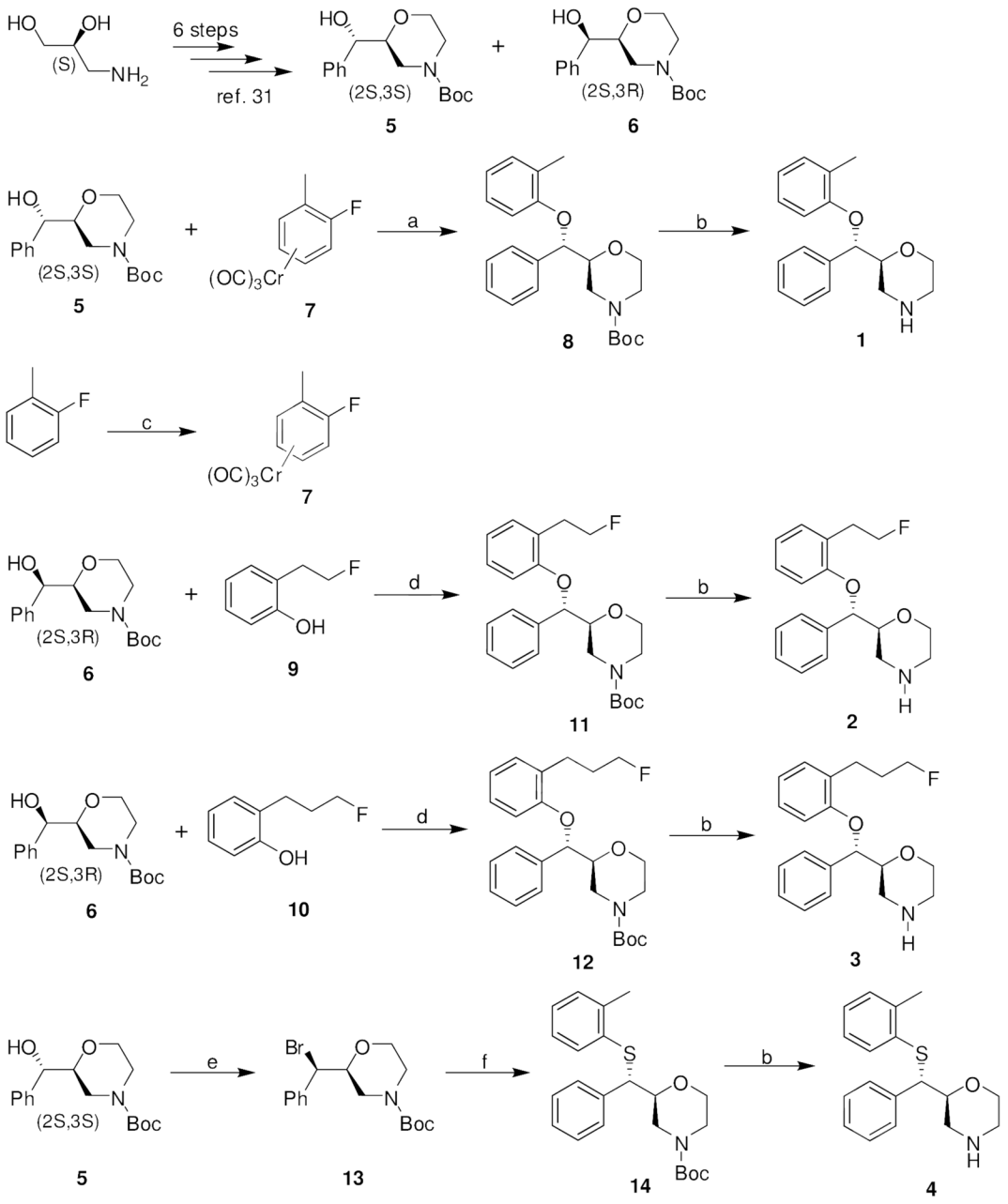

Scheme 1.

Synthesis of the Target Reboxetine Analogs **1, 2, 3**, and **4**a

[a]Reagents and conditions: (a) NaH, DMF, rt, 2 h; I_2, THF, 0 °C to rt, 30 min. (b) TFA, CH_2Cl_2, 0 °C to rt, 2 h. (c) $Cr(CO)_6$, *n*-Bu_2O, THF, reflux, 60 h. (d) DIAD, PPh_3, THF, 0 °C to rt, 48 h. (e) CBr_4, PPh_3, CH_2Cl_2, 0 °C to rt, 30 min. (f) 2-methylbenzenethiol, Cs_2CO_3, DMF, 95 °C, 18 h.

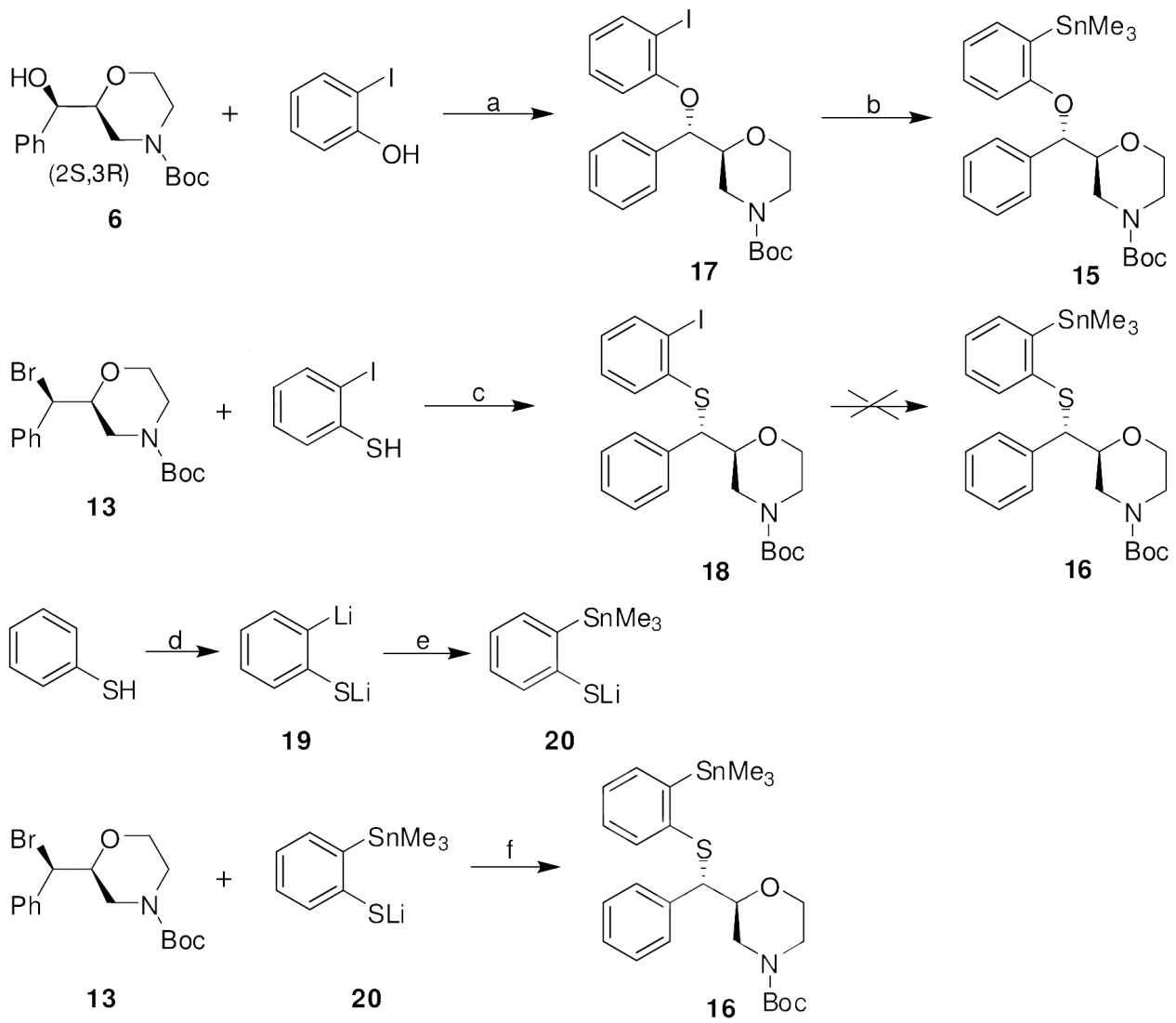

Scheme 2.

Synthesis of the Trimethyltin Precursors for Radiolabeling of [^{11}C]**1** and [^{11}C]**4**a

[a]Reagents and conditions: (a) DIAD, PPh_3, THF, 0 °C to rt, 48 h. (b) $(SnMe_3)_2$, $Pd(PPh_3)_4$, DME, 80 °C, 18 h. (c) Cs_2CO_3, DMF, rt, 18 h. (d) *n*-BuLi, TMEDA, hexane, −78 °C to rt, 24 h. (e) Me_3SnCl, THF, −78 °C, 1 h. (f) Cs_2CO_3, DMF, 100 °C, 18 h.

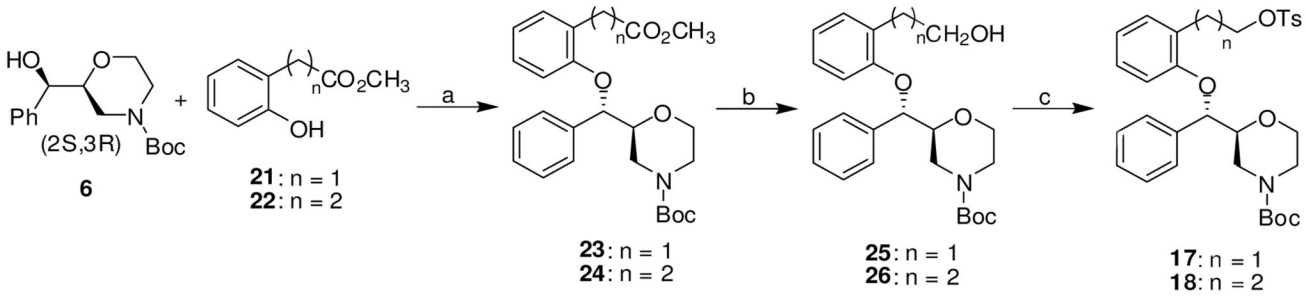

Scheme 3.

Synthesis of the Tosylate Precursors for Radiolabeling of [^{18}F]**2** and [^{18}F]**3**a

[a]Reagents and conditions: (a) DIAD, PPh_3, THF, 0 °C to rt, 48 h. (b) $LiAlH_4$, Et_2O, 0 °C to rt, 30 min. (c) TsCl, Et_3N, CH_2Cl_2, 0 °C to rt, 15 h.

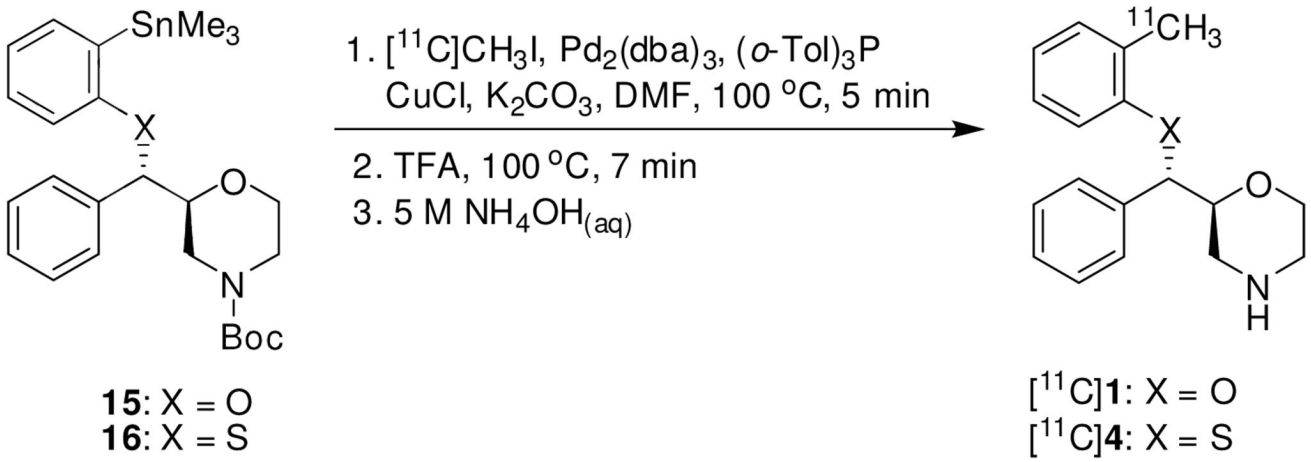

15: X = O
16: X = S

[11C]**1**: X = O
[11C]**4**: X = S

Scheme 4.
Synthesis of [11C]**1** and [11C]**4**

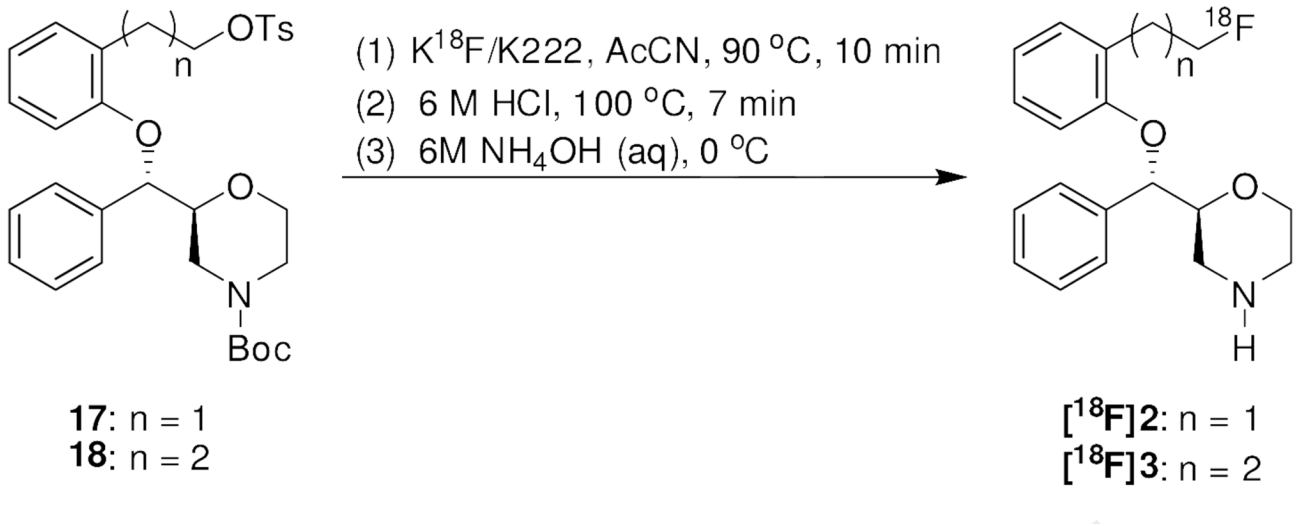

17: n = 1
18: n = 2

[18F]2: n = 1
[18F]3: n = 2

Scheme 5.
Synthesis of [^{18}F]**2** and [^{18}F]**3**

Table 1

Binding Affinities (*K*i (nM)) of Candidate NET Ligands in in vitro Competition Assays with Human Monoamine Transporters[a] and Lipophilicities (log $P_{7.4}$)

compound	K_i for NET[b]	K_i for SERT[c]	K_i for DAT[d]	NET selectivity		log $P_{7.4}$
				SERT/NET	DAT/NET	
MENET, **1**	1.02 ± 0.11	93 ± 20	327 ± 39	92	321	2.04
FENET, **2**	3.14 ± 0.17	430 ± 14	>6000	137	>2000	2.00
FPNET, **3**	3.68 ± 0.92	463 ± 24	>6000	126	>2000	2.29
MESNET, **4**	0.30 ± 0.03	14.80 ± 2.83	275 ± 83	49	917	2.47
(*S*,*S*)-reboxetine	1.04 ± 0.16	661 ± 36	>2000	636	>2000	
(*S*,*S*)-MeNER	0.95 ± 0.03	185 ± 3	>2000	195	>2000	

[a] All K_i values are reported as nanomolar (nM) values. The data are expressed as geometric mean ± standard deviation of at least three separate experiments performed in triplicate.

[b] Competitive binding vs [^{3}H]nisoxetine in HEK-293 cells transfected with human norepinephrine transporters.

[c] Competitive binding vs [^{3}H]citalopram in HEK-293 cells transfected with human serotonin transporters.

[d] Competitive binding vs [^{125}I]RTI-55 in canine kidney cells transfected with human dopamie transporters.

Table 2

Ratios of Uptake of [^{11}C]**1** and [^{11}C]**4** in Brain Regions-of-interest to Caudate at 85 min Postinjection in the Baseline Studies and Pretreatment Studies with Desipramine

	[^{11}C]1			[^{11}C]4	
	Baseline	Desipramine dose (mg/kg)		Baseline	Desipramine dose (mg/kg)
		0.125	0.25		0.125
Thalamus	1.30	1.10	1.06	1.34	1.02
Midbrain	1.43	1.20	0.91	1.33	1.09
Pons	1.44	1.13	0.91	1.27	0.98
Cerebellum	1.25	1.04	0.79	1.05	0.81